Technical Report

Examining Methodological Approaches to Determine the Trace Element Composition in Porewater of Clay Sediments from the Netherlands

Mingkai Ma and Thilo Behrends

Department of Earth Sciences, Utrecht University

Version July 2026

Abstract

Determining the trace element composition in clay formation porewater is essential for assessing radionuclide migration in deep geological repositories, yet remains poorly characterized due to technical challenges in extracting representative samples from low-permeability sediments. We compared three porewater extraction methods (high-pressure squeezing, aqueous extraction, and paper absorption) applied to Dutch Neogene and Paleogene clay cores from 363–406 m depth, analysing 48 trace elements by ICP-MS. Additionally, the trace element composition in piezometer samples from the HADES Underground Research Laboratory (Boom Clay, Belgium) were determined. We focussed in this study on evaluating the validity of the obtained results. This was done by exploring the consistency of measured concentrations with respect to reproducibility and the effect of systematically varied parameters. The latter included the applied pressure during squeezing as well as the solid: liquid ratio, extraction time and bicarbonate addition regarding aqueous extraction.

The reliability of measured trace element concentrations in solutions obtained from high pressure squeezing is challenged due to possible release of metals from the squeezing equipment. Exposing a test solution to the pressure cell resulted in the relative enrichment of the solution, by more than a factor of 10, with the elements Cu, Zr, Hf, Sn. Concentrations of several elements in the squeezed solutions exceeded those in the test solution by more than a factor of 10. Consequently, their abundances in the outflow solution cannot solely be the result of contact with material of the pressure cell and either reflect the porewater composition in the clay or might be an artefact of applying elevated pressure or a consequence of the longer residence time of the solution in the pressure device. For this suit of elements, no plausible explanation for elevated concentrations of Ni and Co could be given and their concentrations might be affected by contamination. Furthermore, concentrations for Sr were questionable as they tend to exceed expected concentrations in equilibrium with $SrCO_3$. Furthermore, a preliminary test indicates that the obtained Se concentrations based on detection of the $^{82}Se^{+}$ ion are unreliable due to interference with $^{81}BrH^{+}$ in the presence of the elevated Br concentrations in the saline solutions.
It turned out that complementary results from aqueous extractions and paper absorption can be helpful in the validation of measured concentrations in solutions

obtained by high pressure squeezing. However, the informative value of measured trace element concentrations in aqueous extracts and solutions obtained from paper absorption are undermined by incomplete separation of solution from solids upon centrifugation and filtration of extracts, or due to attachment of particles to the paper used for porewater absorption. Nevertheless, aqueous extractions indicate that Br behaves quasi conservatively in the investigated clay sediments and the recovered Br originates predominately from porewater. This implies that normalization to Br concentrations opens the possibility to compare results from the different approaches and infer porewater concentrations from paper absorption or aqueous extracts. Next to Br, consistent results were obtained for all three approaches for other elements with relative high abundance in the porewater and, hence, low sensitivity towards unintentional release from solid particles during the extraction procedures. This was, for example, particularly the case for Sr.

In summary, the validation of measured trace element concentrations obtained with the three approaches remained challenging. Only for a few elements the consistency of results from different approaches provide confidence in the measured concentrations. For several elements, cross validation indicates approach-specific alterations of concentrations impeding the reconstruction of the composition of in-situ porewater. However, for most elements, the reliability of measured concentrations remains unclear. Access to groundwater, which could be sampled and analysed with established methods to prevent contamination with trace elements, from aquifers adjacent to the clay-rich sediments, might be of potentially great value for evaluating the reliability and interpreting measured trace element concentrations in the porewaters of clay sediments.

Table of Contents

1. Introduction

1.1 Background

Clay-rich sediments are being investigated in multiple European countries as potential host formations for deep geological repositories of radioactive waste, including Boom Clay in Belgium and the Netherlands (Verhoef & Neeft, 2014; Honty et al., 2022; Wang et al., 2023), Opalinus Clay in Switzerland (Wersin et al., 2024), Callovo-Oxfordian claystone in France (Gaucher et al., 2009; Robinet et al., 2012), and Paleogene clays in the Netherlands (Behrends et al., 2016; Verhoef & Neeft, 2014). These formations function as natural barriers due to their low hydraulic conductivity (typically 10^{-12} m/s, Wemaere et al., 2008), high sorption capacity through cation exchange and surface complexation, and self-sealing properties (Bernier, 2001). Transport in such systems is diffusion-dominated, with advective flow negligible over timescales relevant for radionuclide migration.

Understanding porewater composition in clay formations is essential for performance assessment of geological repositories. Porewater chemistry controls critical processes including radionuclide solubility, speciation, and sorption behaviour (Mazurek et al., 2025). Previous characterization studies of clay formation porewaters have focused primarily on pH, dissolved inorganic carbon, and major cations and anions (Na, K, Ca, Mg, Cl, SO_4) (De Craen et al., 2004; Gaucher et al., 2009; Mazurek et al., 2025). However, trace element composition of porewater in clay-rich sediments remains poorly characterized, with only limited trace element data available from a few European clay formations (De Craen et al., 2004). This knowledge gap is significant for assessing radionuclide migration behaviour.

1.2 Importance of trace element characterization of porewaters from clay-rich formations

Determining trace element composition in clay porewaters can provide useful information for the performance assessment of radioactive waste disposal. Some radionuclides, which are present in the waste forms, also occur naturally within the host formation and the corresponding porewater. This group includes ^{283}U and ^{232}Th. For other long-lived radioactive fission products such as ^{135}Cs or ^{79}Se, stable isotopes occur naturally in the host formation. Finally, some naturally occurring trace elements are conceived as chemical analogues to radionuclides, potentially included in the

waste. That is, the geochemical behaviour of the chemical analogue in the natural environment is expected to be similar to that of the radionuclide due to similar electron configuration, ionic radius, stereo- or redox chemistry. Examples include Re as an analogue for Tc (Kim and Boulègue, 2003) or Eu(III) as an analogue for trivalent actinides, in particular, Am(III) and Cm(III) (Lakshtanov and Stipp, 2004). Understanding of the processes controlling the natural concentration of these trace elements in porewater, can, therefore, shed light on the migration of radionuclides in the host formation. In particular, binding and release of these elements to or from the solid phase at relevant concentrations and time scales is of great relevance for the safety assessment of radioactive waste disposal. For determining the apparent distribution coefficient of naturally occurring trace elements in the host formation, the activities in the porewater as well as in the solid-bound pool need to be known. Solid-bound pools include, for example, the cation exchange complex, reactive sites at mineral surfaces, or the bulk composition of minerals, for which the reaction kinetics of structural exchange with the aqueous phase is fast enough to significantly affect porewater chemistry within the relevant time scale (e.g. time scales of molecular diffusion, convective water flow or radioactive decay). While identification of relevant reactive phases or pools and the corresponding trace element activities might be challenging, determination of trace element activities in the host formation's porewater is a the first step in determining the apparent distribution coefficients.

1.3 Approaches to determine porewater compositions

A straightforward approach to determine the composition of porewaters is to firstly extract the porewater and then determine its composition by analytical methods. However, the small particle size in clay-rich sediments results in a pore size distribution with a small median diameter. Consequently, strong capillary forces hamper the extraction of porewater from clay-rich sediments. This fundamental problem require the development of specific methods for measuring the composition of porewater in clays. Several approaches have been applied to determine the porewater composition in clay-rich formations including, 1) In situ collection of porewater from piezometers; 2) Advective displacement (Kiczka et al., 2023) ;3) High pressure squeezing (Fernández et al., 2004; Mazurek et al., 2015; Wersin et al., 2022); 4) Paper absorption (Celejewski et al., 2014, 2018) and; 5) Aqueous extraction.

In situ collection of porewater with piezometers requires direct access to the clay-rich formation and for deep formations the necessary infrastructure is provided only in underground research laboratories (URL) such as HADES in Belgium (Hassine et al. 2023). The other approaches can be applied to undisturbed material collected from the formations, for example from core drilling. For high pressure squeezing and advective displacement dedicated technical equipment is required and the techniques are only available at some laboratories in the world. In contrast, paper absorption and aqueous extraction do not require very sophisticated apparatuses as long as sample preparation and application of the method can be done by avoiding changes in the redox state of the sample. The goal of the first four approaches is to separate the porewater from the solids without altering its chemical composition. In contrast to the other methods, aqueous extraction inherently involves the perturbation of porewater composition due to dilution and bringing part of solid-bound pool into solution.

However, all these approaches to obtain porewater from low-permeability clay-rich sediments present substantial technical challenges (see Mazurek et al., 2025 and references therein). The chemical composition measured in extracted porewater may deviate significantly from in situ conditions due to: (1) oxidation artifacts during sample handling affecting redox-sensitive elements, (2) mineral dissolution or precipitation induced by pressure application or dilution, (3) cation exchange reactions triggered by altered solid:water ratios, (4) CO_2 outgassing affecting carbonate equilibria and pH, and (5) colloidal mobilization (Mazurek et al., 2025).

For trace element analysis specifically, additional challenges are posed due to possible contamination or loss of trace elements upon the reaction with material used in the procedures. Different extraction methods may introduce element-specific artefacts that are negligible for major elements but significant for trace constituents. For example, high-pressure squeezing through steel equipment can contaminate samples with Fe, Cr, Ni, Mo, and Mn. Extended equilibration in aqueous extraction experiments allows slow dissolution of trace-bearing accessory minerals (for example pyrite or apatite) that do not alter major element concentrations significantly but can strongly increase trace element concentrations. Furthermore, analytical methods with ng/L detection limits are required to quantify trace elements concentrations (Li et al., 2023). The detection limit of the analytical technique might be crucial when the

porewater becomes diluted upon aqueous extraction or when dilution is required when the porewater has high electrolyte concentrations (saline or hypersaline solutions) interfering with the analytical method such as inductively coupled plasma mass spectrometry (ICP-MS). Additionally, spectral interferences can undermine the reliability of measured trace element concentrations by ICP-MS.

1.4 Objectives

In this study different approaches to determine trace-element concentrations in Paleogenic clay-rich formations in the Netherland and Belgium were tested. Next to trace element analyses of porewater from the HADES URL, three approaches were applied to samples obtained from one Neogene and two Paleogene clay formations. The approaches included high-pressure squeezing, aqueous extraction, and paper absorption. The study focussed on the effect of methodological parameters on trace element composition. The study aims at creating a starting point for identifying the potential and possible limitations of the different approaches to determine trace element compositions of the formation's porewater. A crucial aspect hereby is the critical assessment of the validity of the measurements and the discussion of possible artefacts.

2. Materials and methods

2.1 Material from Paleogene and Neogene clay-rich formations

This study investigates samples from two Paleogene and one Neogene clay formations in the Netherlands. Core samples were obtained from borehole DAPGEO-02 drilled as part of the Delftse Hout geothermal research project to depths of 500 m below surface (Vardon et al., 2024). These formations represent marine clay deposition under varying conditions. The Ieper/Ypresian clays correspond to formations being studied by ONDRAF/NIRAS in Belgium as potential disposal horizons.

Three cylindrical core samples (diameter 100 mm, length ~120 cm each including case and wax sealing) were received from TU Delft and immediately transferred to 4°C storage in the Earth Sciences Laboratory cold room facility at Utrecht University (UU).

These cores were collected between February to May 2022 using the Smet Coring System. The cores were retrieved as part of the drilling of the Delftse Hout multipurpose research borehole DAPGEO-02 (Vardon et al., 2024) at Tweemolentjeskade in Delft, The Netherlands. This drilling campaign has been executed in the context of the Geothermal Delft project led by Delft University of Technology.

Cores were maintained in their original PVC liners sealed with end caps and plastic wrap to prevent moisture loss and oxidation until processing. The samples represent three geologically distinct formations from borehole DAPGEO-02 (Table. 1).

Table. 1 Sample information used in this study.

Core name	**Formation**	**Depth(m)**
DAPGEO-02-C20	Diessen	363.40 – 364.10
DAPGEO-02-C57	Dongen, Ieper member	392.66 – 393.66
DAPGEO-02-C75	Landen/Liessel Formation	405.11 – 406.11

Prior to transferring cores to UU, high-resolution computed tomography (CT) scans of intact cores were performed at TU Delft (Fig. 1).

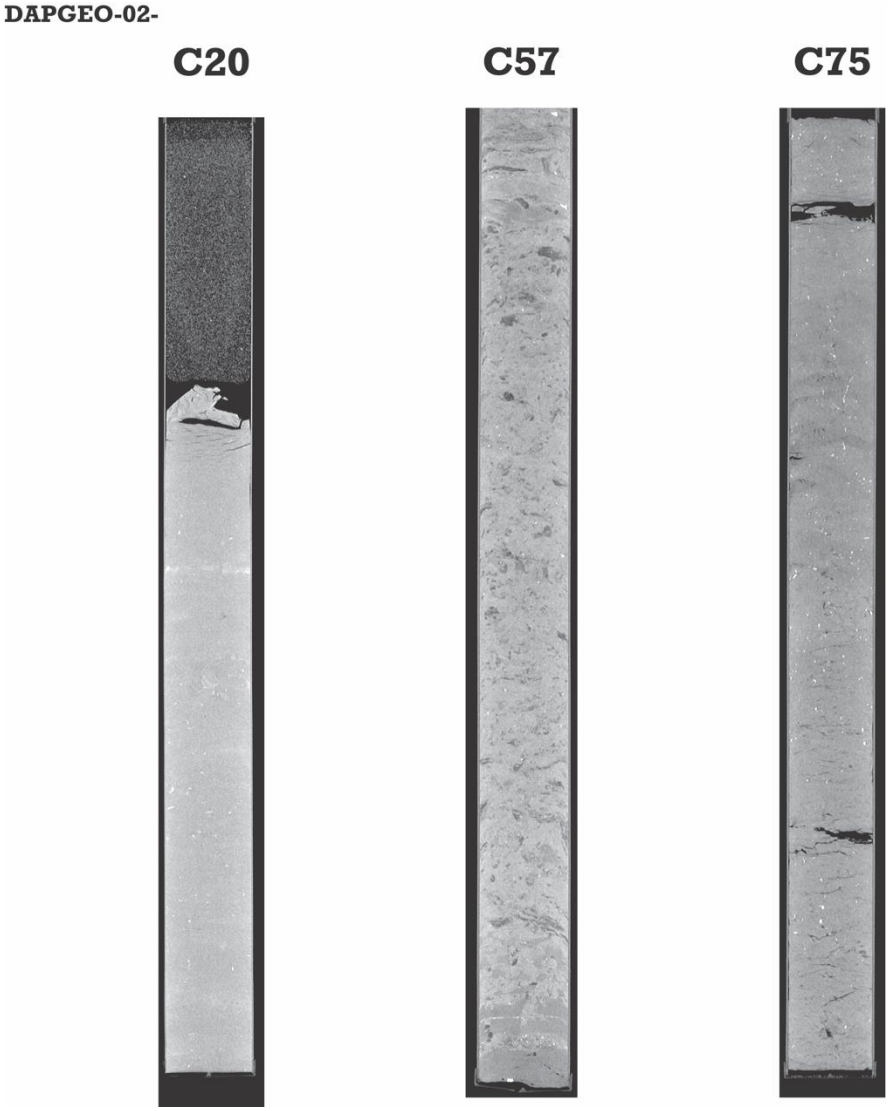

Fig. 1 High-resolution computed tomography (CT) scans of the three cores(DAPGEO-C20, DAPGEO-C57 and DAPGEO-C75)

2.2 Sample preparation

2.2.1 Core handling

All core opening, sectioning, and subsampling procedures were conducted inside a custom-built anoxic glove box filled with N_2/H_2 (95%/5%) and equipped with a platinum-catalyst oxygen-removal system to prevent oxidation artifacts. As the cores are longer than the transfer chamber of the glove box, the glove box was opened before transferring each core into the glove box. Afterwards, the box was closed again, flushed with N_2 for 24 hours, and subsequently, the gas was switched to N_2/H_2 (95%/5%). Core handling was conducted until the oxygen level was below 1 ppm. Prior to core slicing, cores were carefully marked on exterior surfaces to ensure unequivocal

identification of each core section as well as their orientation. For the core slicing, a cast saw was used to cut the PVC liners open. Subsequently, corresponding sections were divided using a ceramic knife. For more indurated intervals gentle hammer was applied.

Based on CT scan analysis and experimental design, each selected 20 cm core interval was subdivided into several portions for the different approaches. A 10 cm section for high-pressure squeezing was selected from the most homogeneous interval and maintained as an intact cylinder to preserve in situ structure. Three 1 cm sections for aqueous extraction were distributed systematically along the 20 cm interval to assess spatial reproducibility and detect potential heterogeneity. Two 2 cm sections for paper-absorption were selected from intervals bracketing the squeezing section.

The subsamples were transferred to pre-labelled plastic zip-lock bags, with excess atmospheric gas manually expelled before sealing to minimize headspace. Sealed sample bags were immediately enclosed in two-layered aluminium foil bags with integrated zip seal, and later hot sealed. Samples were immediately transferred to 4°C cold storage until further use. Core sections not used for porewater extraction were retained sealed and archived at 4°C for potential future solid-phase characterization (XRD mineralogy, XRF etc, see Hoving et al., 2025).

Table. 2 Pictures and description of core slices used fin this study. The name of the sample shows the sections during slicing (see Fig. 3). Additional pictures obtained from the preparation of other cores for high pressure squeezing are available in the appendix.

Pictures	Description
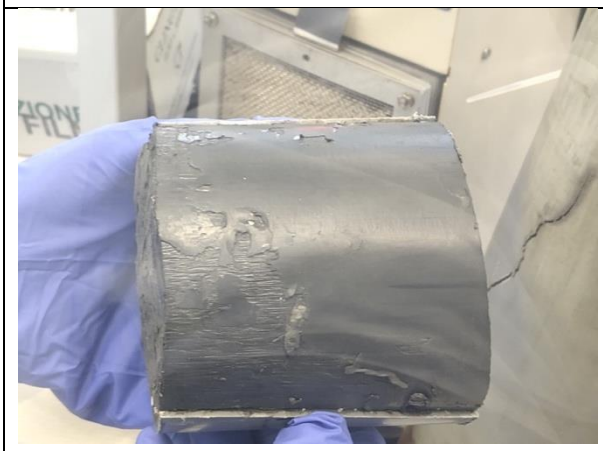	Freshly opened core (C20-P4).
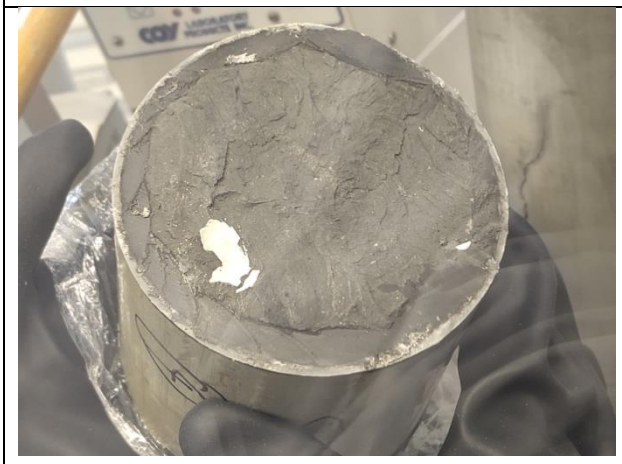	Freshly opened core, with a fossil shell (C20-P4-0cm).
	Core DAPGEO-C20, the upper opening was filled with sand, and sealed with wax.

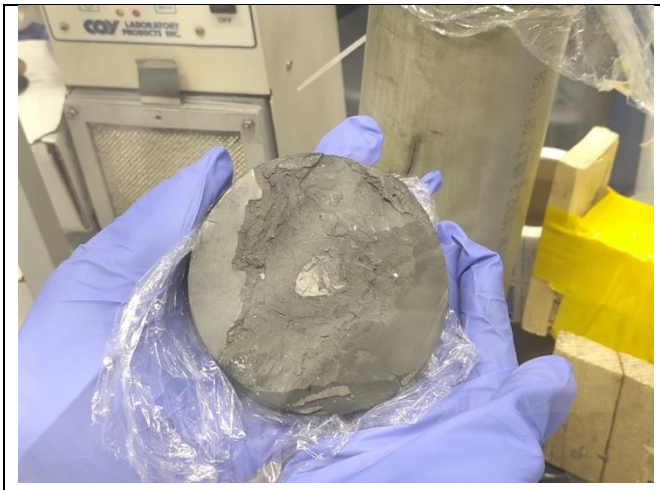	The sliced core DAPGEO-C20-P4-6-8cm.
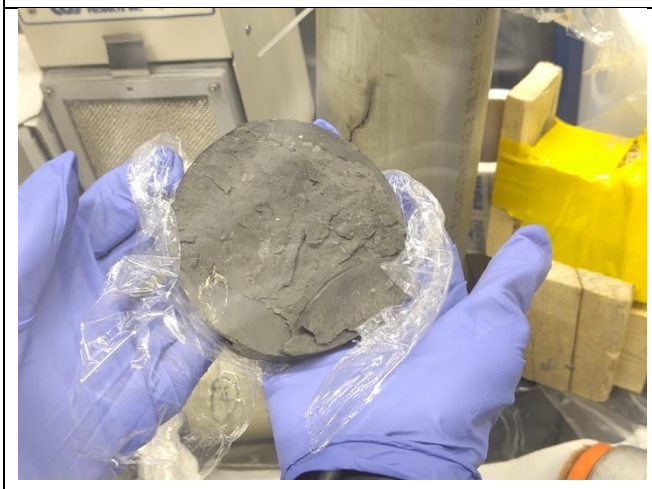	The sliced core DAPGEO-C20-P4-2-4cm.
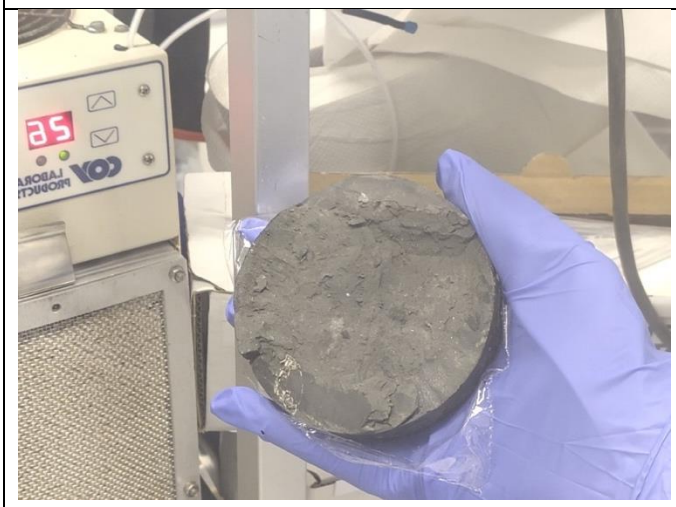	The sliced core (2cm).

	Sliced core, sample used for aqueous extraction (DAPGEO-C20-P4-4-6 cm)
	Sliced core, sample used for aqueous extraction (DAPGEO-C20-P4-8-10 cm)

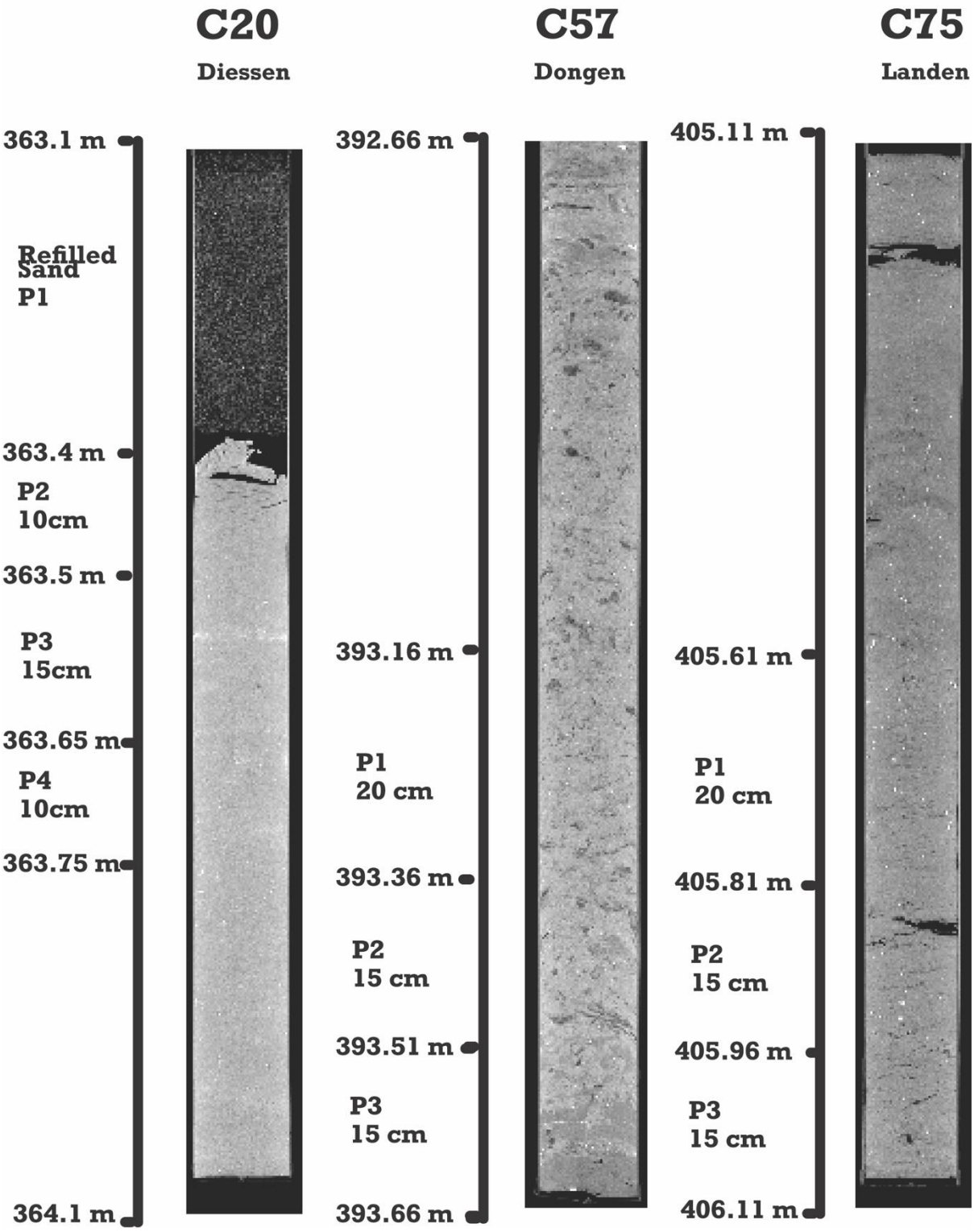

Fig. 2 CT scans showing subsampling scheme for the three formations. Sample nomenclature indicates core number, section (P1-P4), and depth interval from section start (e.g., DAPGEO-C20-P1-2-4 cm represents C20, section P1, 2-4 cm interval).

2.3 Porewater extraction methods

2.3.1 High-pressure squeezing extraction

Three intact 10 cm core sections (one from each core) were shipped to CIEMAT (Centro de Investigaciones Energéticas, Medioambientales y Tecnológicas), Madrid, Spain, for high-pressure squeezing extraction. High-pressure squeezing exploits the mechanical compressibility of water-saturated porous media. Application of uniaxial stress exceeding in situ effective stress induces pore volume reduction, forcing mobile porewater through filter membranes while retaining solid matrix (Fernández et al., 2004; Fernández and Villar, 2010; Mazurek et al., 2015).

The high-pressure squeezing procedure followed established protocols from CIEMAT laboratory. Prior to squeezing, the pressure chamber and the connected tubing was flushed with a test solution used internally at UU as a seawater matrix. This was done to assess the possibility of contamination by the material in the squeezing device and the connected tubing. Cores were squeezed at different pressures, varying from 5 Mpa to 50 Mpa. This was done to investigate the effect of pressure on trace element composition. The retrieved porewaters were subsequently filtered (0.2 µm) and acidified with HNO_3 (10%) until further analysis.

Additionally, porewaters retrieved from five other cores were also analysed for trace element composition. The cores included DAPGEO-C27, DAPGEO-C39, DAPGEO-C55, DAPGEO-C62, and DAPGEO-C71 and the porewater was collected for constraining the geophysical investigations at the TUDelft.

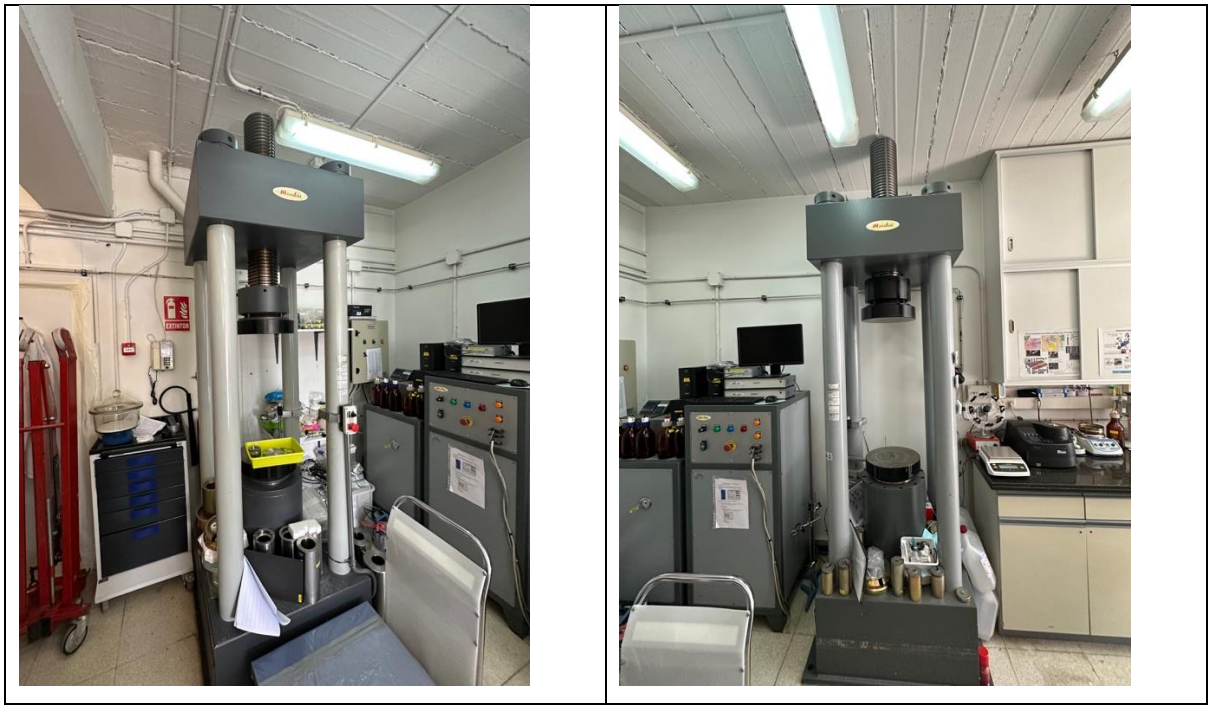

Fig. 3 High-pressure squeezer at CIEMAT.

2.3.2 Aqueous extraction

Aqueous extraction was performed on twelve 1 cm thick core sections (four per core). The procedure was based on protocols adapted from Nagra technical report NAB 20-13 (RWI, 2020) and De Craen et al. (2004).

Preliminary optimization tests were conducted to determine optimal extraction conditions. Core sections were tested with four different solid:liquid ratios (1 g/L, 25 g/L, 50 g/L, and 200 g/L) using three different solutions: deionized water, 0.1 M $NaHCO_3$, and artificial seawater (Instant Ocean). Based on these preliminary results, two solid:liquid ratios (25 g/L and 200 g/L) and two solutions (deionized water and 0.1 M $NaHCO_3$) were selected for the main experimental program. Additionally the extraction time was varied to assess the temporal evolution of trace element composition. The investigated reaction times were 1 day, 7 days, and 28 days. All extractions were performed in duplicate.

Prior to the addition to the core material, deionized water (conductivity < 18.2 MΩ·cm) was degassed by vigorous bubbling with N_2 gas for minimum 60 minutes in order to remove dissolved oxygen. For $NaHCO_3$ experiments, 0.1 M $NaHCO_3$ solution was prepared using degassed deionized water and the pH was adjusted to approximately 8.12, corresponding to equilibrium with Boom Clay reported pCO_2 conditions (De Craen et al., 2004; Behrends et al., 2016).

Corresponding core sections were unpacked inside the glove box (as described above) and manually disaggregated. Weighed amounts of disaggregated clay were transferred into 50 mL PP centrifuge tubes and the appropriate volume of degassed solution (deionized water or 0.1 M $NaHCO_3$) was rapidly dispensed to achieve the target solid:liquid ratios of 25 g/L or 200 g/L. Tubes were immediately capped and vortexed thoroughly to homogenize the clay-solution suspension. All tubes were then put onto a horizontal shaker inside the anoxic chamber. Suspensions were constantly agitated (120 rpm) at for the designated contact times of 1 day, 7 days, or 28 days.
At each sampling interval, samples were removed from the glove box and centrifuged at 2700 x g for one hour to achieve phase separation. After centrifugation, tubes were transferred back into the glove box where the supernatant was carefully decanted. The solutions were filtered sequentially, first through 0.45 µm and then through 0.2 µm nylon membrane syringe filters (mdi). The filtered solutions were acidified with 10% HNO_3. Both solutions and solids were stored at 4°C until further analysis.

2.3.3 Paper-absorption method

Six core sections (~2 cm thick, one pair per formation) were used for testing the cellulose paper absorption approach following Celejewski et al. (2014, 2018). Selected 2 cm core sections were carefully split longitudinally inside the anoxic glove box using a sharp ceramic knife. Then a Whatman No. 1 CHR cellulose filter paper (100 mm diameter) was positioned on one freshly split core half in the petri dish. The second core half was aligned and pressed firmly against the paper. Reassembled cores were immediately wrapped in multiple layers of vinyl tape to maintain compression and prevent core separation, then secured with rubber bands. Wrapped cores were placed in individual sealed plastic bags, then enclosed in double-layer aluminium foil bags and stored at 4°C for a two-month equilibration period. The samples were contained in both glass petri dishes and 3D-printed petri dishes (PLA material) with enhanced physical texture to evaluate potential improvements in clay-paper contact and porewater transfer efficiency.
After two months, sealed packages were transferred back into the anoxic chamber and papers were carefully extracted using tweezers. Papers were visually examined for indications of water absorption, adhering clay particles, discoloration, and structural integrity. The retrieved papers were immediately weighed. Each paper was transferred

to a clean, acid-washed 50 mL polyethylene centrifuge tube containing 15.0 mL deionized water (acidified with 1% HNO_3), and placed on an orbital shaker (120 rpm) at room temperature for 24 hours to extract absorbed solutes. After leaching, papers were removed and gently pressed against the tube wall to recover entrained water. Leachate solutions were filtered through 0.2 µm syringe filters and preserved following identical protocols as aqueous extraction samples for further analysis.

2.4 Porewater obtained from the HADES URL

Porewater samples from Boom Clay were obtained from the HADES URL operated by EIG EURIDICE in Mol, Belgium. The HADES facility provides access to in situ Boom Clay formation at approximately 225 m depth, where porewater was collected via piezometers installed in the formation. Porewater collection was done according to established protocols at the HADES URL (Honty et al., 2022). After sampling, the porewater was split into two fractions. One fraction acidified with HNO_3 immediately upon collection while the other fraction remained unmodified. This was done to test the effect of acidification on trace element concentrations. Acidification is expected to prevent the oxidation of Fe^{2+} by atmospheric oxygen but could lead to the dissolution of colloidal particles. Additionally, ultrafiltration was applied to selected porewater samples using Amicon® Ultra Centrifugal Filter units (3 kDa molecular weight) to distinguish between truly dissolved species and colloid-associated elements. Ultrafiltration was performed with a 12 mL subsample of the solutions and via centrifugation at 3000 g for 1 hour.

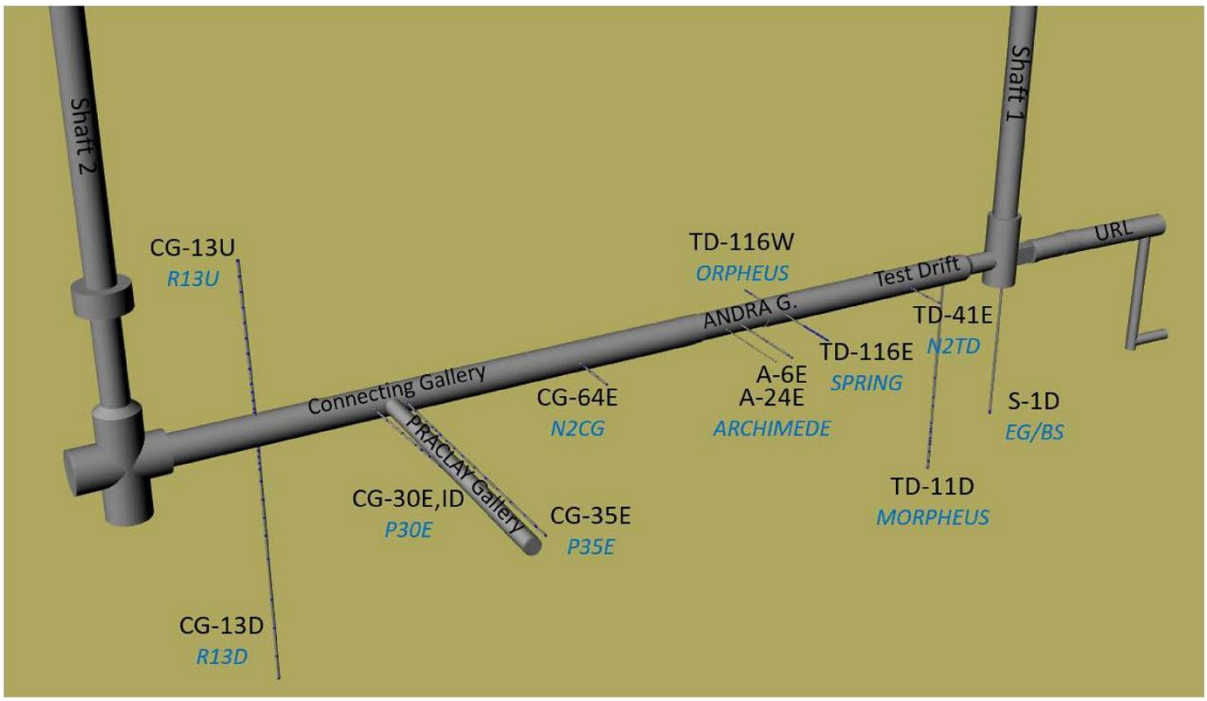

Fig. 4 Technical conceptual figure of the piezometers in the HADES underground research laboratory (cite from De Craen et al., 2023). Water samples were collected from the CG-13U, CG-13D and the TD-116E piezometers.

2.5 Analytical methods

2.5.1 Water content analysis

Water content of clay samples was determined gravimetrically by oven-drying at 105 °C until constant weight was achieved. Samples were weighed before and after drying using an analytical balance, with weight measurements repeated at regular intervals until the change between successive measurements was less than 0.1%. Water content was calculated as the ratio of the mass of free water to the mass of dry soil according to:

$$w_r = \frac{m_{wet} - m_{dry}}{m_{dry}} * 100\%$$

where w_r is the water content (wt%), m_{wet} is the initial wet mass, and m_{dry} is the mass after drying at 105°C.

The measured water contents were 23.1 ± 0.1 wt% for the Diessen Formation (DAPGEO-C20), 18.9 ± 0.3 wt% for the Dongen Formation (DAPGEO-C57), and 27.6 ± 0.1 wt% for the Landen Formation (DAPGEO-C75).

2.5.2 Trace element analysis by ICP-MS

Trace element concentrations in porewater samples were determined by Inductively Coupled Plasma Mass Spectrometry (ICP-MS) using a PerkinElmer NexION 2000p ICP-MS at the UU GeoLab. Acidified samples (preserved with 1% HNO_3) were analysed for 48 trace elements: Li, Be, Sc, V, Cr, Mn, Fe, Co, Ni, Cu, Zn, As, Br, Se, Rb, Sr, Y, Zr, Nb, Mo, Cd, Sn, Sb, Cs, Ba, La, Ce, Pr, Nd, Sm, Eu, Gd, Tb, Dy, Ho, Er, Tm, Yb, Lu, Hf, Ta, W, Re, Ag, Tl, Pb, Th, and U. The elements Sc, V, Cr, Mn, Fe, Co, Ni, Cu, Zn and As were measured in He collision mode with kinetic energy discrimination (KED), while all other elements applying the standard mode. Nevertheless, spectral interferences can occur. In particular, measuring Se concentrations in the saline matrix based on the $^{82}Se^{+}$ ion turned out to be biased due to $^{81}BrH^{+}$ interference (see appendix for details). For this reason, the reported Se concentrations in the saline matrix are considered to be unreliable and are ignored in this report.

All samples were acidified and filtered prior to analysis, with dilution applied as necessary to bring concentrations within the optimal analytical range and to minimize matrix effects. Multi-element calibration standards were prepared from certified reference solutions to cover the expected concentration ranges. Internal standards were added to all samples and standards to correct for instrumental drift and matrix effects during analysis.

3. Results and discussion

3.1 Solutions from HADES piezometers

Trace element concentrations in waters from HADES piezometers(Fig. 5) span approximately seven orders of magnitude, from below detection limit (<1 parts per trillion) to >10^3 µg/L. Within the group of measured elements from piezometer samples in this study, Fe concentrations were highest with an average value of 319 and 288 ppb for acidified (a) and non-acidified (na) samples, respectively. Regarding average concentrations, the other most abundant elements were Sr (43.3 (a)/ 42.9 (na) ppb), Zn (50.1 (a)/ 34.8 (na) ppb), Li (34.8 (a)/ 35.1 (na) ppb), Ba (34.4 (a)/ 12.1 (na) ppb), and Mo (14.7 (a)/ 13.8 (na) ppb).

The patterns of elemental concentrations were similar among the piezometer samples. Noticeable were the systematically higher concentrations for lanthanides and several other elements, including U and Eu, in solutions from piezometer CG-13D-4. Another obvious feature is the exclusive detection of W in samples from TD-116E and in the acidified sample from CG-13D-4. Apart from these observations, no consistent trend could be detected when comparing elemental concentrations between the different piezometers.

Among the elements with average concentrations above 1 µg/L, the coefficient of variation varied between 16.6 and 125.9% for non-acidified and 19.3 and 239.3% for acidified samples. Concentrations of Rb (19.2% (a) 16.6% (na)), Sr (43.3% (a) 36.3% (na)), Mo (57.7% (a) 39.2% (na)) variation was smallest, while the largest variation was obtained for the elements Cr (111.9% (a) 125.9% (na)), V (136.5% (a) 123.4% (na)) and Cu (154.9% (a) 118.6% (na)).

Br concentrations were only included in the analysis of ultrafiltrated samples. The average concentration was 430 ± 190 µg/L. Based on the test (see appendix), the average Br concentration contributes to the determined Se concentration by about 1 µg/L due to ^{81}BrH interference. The average Se concentration including all acidified and non-acidified samples was 3.4 ± 3.0 µg/L implying that the bias due to spectral interference in the fresh water from the HADES piezometer is considerably smaller compared to saline waters from the Dutch samples. However, Se is an element exhibiting large coefficients of variation and differences between acidified and non-acidified piezometer samples, hence being compromised by relatively large analytical

uncertainty. That is, the informative value of the measured Se concentrations is also restricted for the samples from the HADES piezometers.

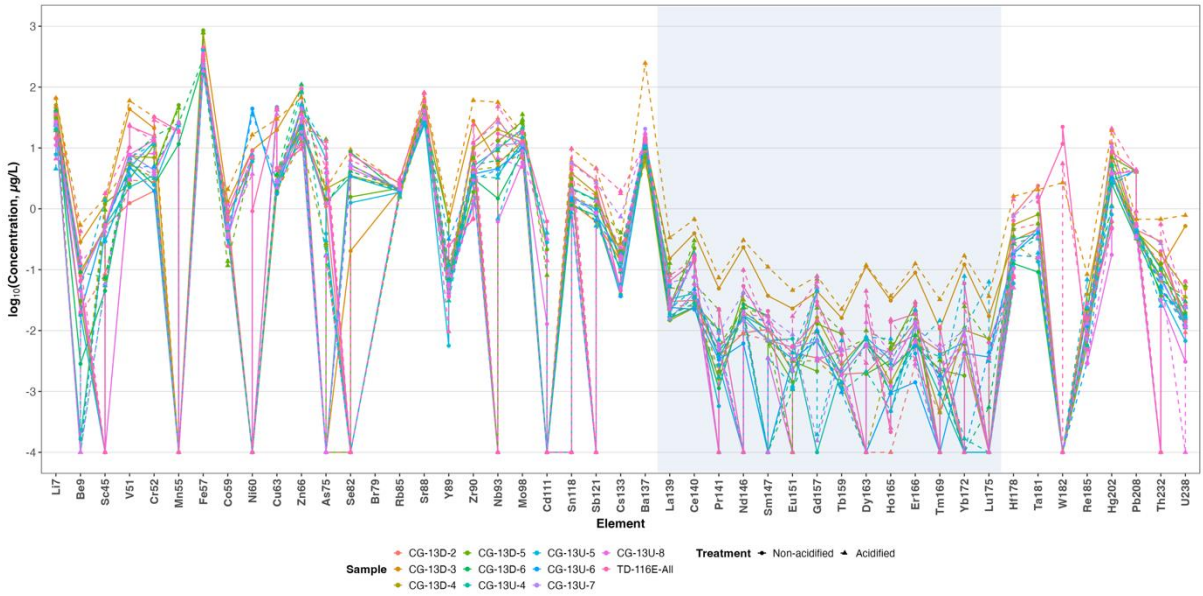

Fig. 5. Trace element concentrations in porewater samples collected from various piezometers at the HADES URL. Data are presented as $\log_{10}$ (concentration, µg/L). Acidified samples are shown with square symbols, non-acidified samples with triangle symbols. The shaded area shows rare earth elements (REEs) from La to Lu. Each coloured line represents a different piezometer sample location within the Boom Clay formation (see Fig. 4).

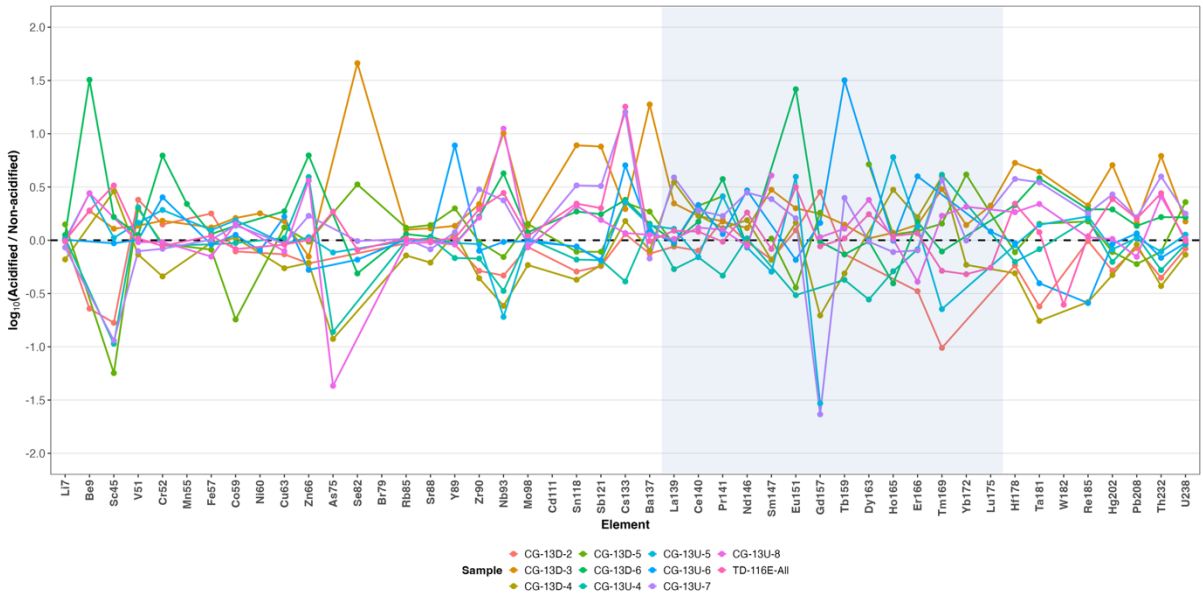

Fig. 6 Effect of acidification on trace element concentrations in HADES porewater samples ($\log_{10}$ concentration ratios of acidified to non-acidified samples). Values above the dashed zero reference line indicate higher concentrations in acidified samples, while values below indicate higher concentrations in non-acidified samples. The shaded area shows rare earth elements (REEs) from La to Lu. Each coloured line represents a different piezometer location. Log ratios near zero indicate minimal acidification effect.

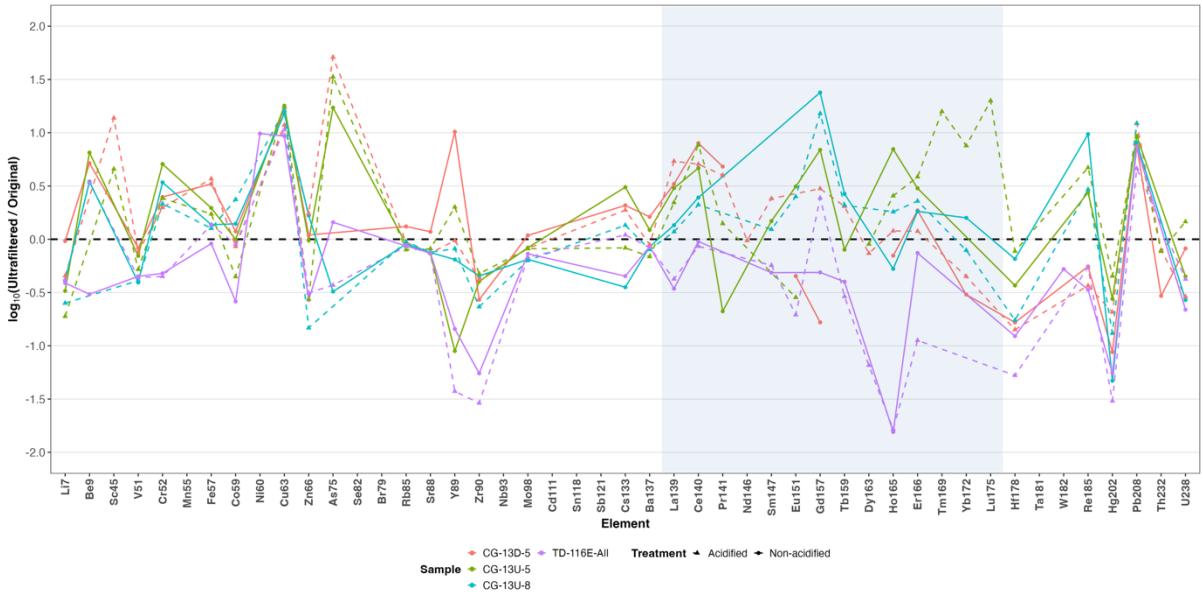

Fig. 7 Effect of ultrafiltration on trace element concentrations in HADES porewater samples ($\log_{10}$ concentration ratios of ultrafiltered to original samples). Samples were ultrafiltered using 3 kDa molecular weight cutoff membranes. Negative values indicate element removal during ultrafiltration, suggesting colloidal or particulate association (>3 kDa), while positive values indicate enrichment in the ultrafiltered fraction. The shaded area highlights lanthanides. Each line pair represents a different piezometer location, with solid and dashed lines representing non-acidified and acidified samples, respectively.

Acidification directly after sample collection did not have a consistent effect on elemental concentrations (Figs. 5 and 6). With the exception of a few outliers, concentrations after acidification were less than 10 times larger or lower with random deviations from a ratio of one to higher and lower ratios (Fig. 6). Random variation from a ratio of one suggests that the observed fluctuations originate from random errors related to sample collection, handling and analysis. This implies that acidification was not necessary for sample preservation in order to prevent precipitation of solids (e.g carbonates), oxidation artefacts (e.g. oxidation Fe^{2+} or Mn^{2+}) or adsorption to the container. Furthermore, absence of a consistent trend in concentration after acidification further indicates, that acid-induced dissolution of or desorption from particulate matter had not affected trace element concentrations. This, in turn, implies that the sampled water did not contain significant amounts of acid-labile, particle-bound trace elements due to effective retention by the filter screens of the piezometers or their absence in the infiltrating porewater.

Ultrafiltration through 3 kDa molecular weight cutoff membranes (Fig. 7) distinguishes truly dissolved species and small polynuclear complexes (<3 kDa, approximately <2 nm diameter) from trace elements bound to organic and inorganic colloids. However, only for a few elements, pronounced depletion in the sample after ultrafiltration was consistently reflected in negative log ratios (in Fig. 7). This was the case for Zr, Ho, and Hg, whose concentrations decreased up to a factor of about 30 upon ultrafiltration ($\log_{10}$ ratios up to -1.5), Note, the decrease in concentration can also be caused by sorption to the membranes and material in the centrifuge tubes.

In contrast, the concentration of some elements consistently increased upon ultrafiltration. A pronounced increase in concentration in the filtrates by up to an factor of 10 was obtained for the elements Cu and Pb. Also the concentrations of As, Sc, and Gd showed a pronounced enrichment in most ultrafiltered samples. An increase in concentration can be ascribed to contamination during ultrafiltration. For Mn, concentrations were not reported for the solutions before ultrafiltration and, hence, the affect of ultrafiltration cannot be assessed. The reason for the lacking of Mn in the analytical report remains unclear. Furthermore, results from blank filtrations were not available and in future research possible contamination of samples due to ultrafiltration should be evaluated using blanks.

For the other elements, the trends were inconclusive and for some samples concentrations increased upon ultrafiltration while they decreased for others. For these elements a possible effect of ultrafiltration on concentration might be masked by analytical uncertainties. However, when comparing piezometers, concentrations after filtration were systematically lower for piezometer TD-116E, the SPRING piezometer, with the exception of elements showing indications for contamination artifacts. The design of this piezometers differs from that of the others, which could result in a larger fraction of colloidal particles in the retrieved water. As the decrease occurred similarly for acidified and non-acidified water samples, the particles are apparently stable in acid solution and do not release the associate trace elements upon acidification. It is plausible that this water contains clay minerals and their removal can account for the decrease in trace element concentration. For the other piezometers, the absence of a consistent depletion of trace elements upon ultracentrifugation suggests that the fraction of particle-bound trace elements was only of minor importance in the retrieved samples possibly by effective retention by the filter screens or a low contribution of suspended particles to the trace element transport in the sampled layers.

In conclusion, the results do not provide indications for alterations in trace element composition upon porewater collection using piezometers, in particular of the vertical CG13-D and CG13-U piezometers. The uniformity in trace element concentrations in waters of these filters, the absence of erratic fluctuations (a potential indication for contamination), and the insensitivity of most element concentrations towards acidification and ultrafiltration suggest that the water retrieved from these piezometers represents concentrations of truly dissolved trace elements in the sampled clay and silt layers.

3.2 High-pressure squeezing

High-pressure squeezing was applied to intact core sections from six different depths spanning various formations. For three samples, sequential extraction at increasing pressures (5 to 50 MPa) allowed examination of how applied pressure affects porewater composition.

The general elemental concentration patterns of the collected water from most samples and at most pressures were very uniform (Fig. 8). One notable exception is sample from core C62 at 20 MPa, which showed substantially higher concentrations than all other samples, particularly for the elements Fe, Mn, Cr, Ni, Co, Mo and the lanthanides.

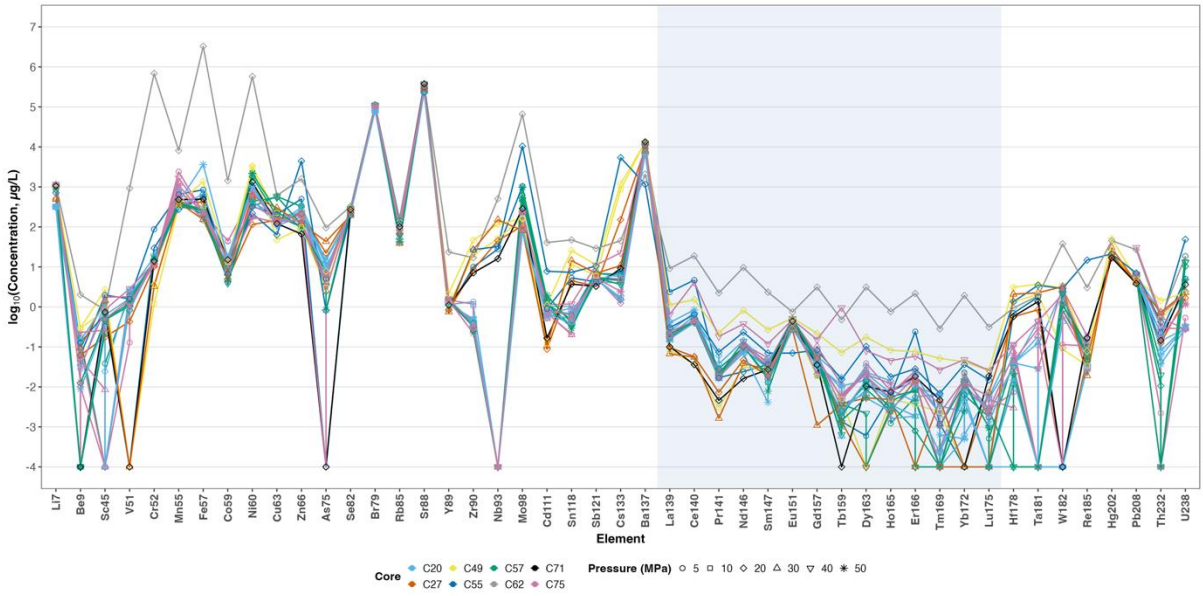

Fig. 8 Trace element concentrations in porewater obtained by high-pressure squeezing ($\log_{10}$ scale, µg/L). Sequential extractions were performed at increasing pressures from 5 to 50 MPa. Each coloured line represents a different core sample. The shaded area highlights lanthanides from La to Lu. Different

symbols indicate applied pressure for each collection step. Note, the reported Se concentrations are not reliable due to spectral interferences (see appendix).

Variability of concentrations among samples (when excluding sample C62) was smallest (coefficient of variation < 50 %) for elements Br, Sr, Rb and Li. Other elements showed high variability with concentrations spanning two orders of magnitude including most of the lanthanides (with the exception of Eu) U, Th, Cs, Mo and Sc.

In order to obtain further indications about the reliability of measured trace element concentrations and factors affecting the variability, the variation among measurements was investigated in more detail. From the squeezing experiment, in total, 14 solutions were obtained. Each solution was measured in duplicate and the difference between the results reflects analytical uncertainty. In Fig. 9, the median of the ratios between the absolute difference of duplicate analyses and the corresponding average concentration are presented as a function of the average concentration for all solutions and replicates (blue colour). For all elements, with the exception of V and As, with an average concentration above 1 µg/L, the median relative difference in duplicate measurements was below 10 %. The divergently large uncertainty of As analysis using ICP-MS can be ascribed to interference with the $ArCl^+$ ion formed in the plasma with similar mass as As . This is a particular problem for the Cl-rich matrix of the porewater, investigated in this study. Hence, similarly as for Se, for accurate As analyses by ICP-MS extra measures need to be taken.

The variation between duplicate measurements tends to increase with decreasing concentration reaching relative differences above 60 % for the elements with average concentrations in the lower ppb range. In some cases, the element was not detected in one measurement. Assigning a value of zero in this case leads to a 200 % deviation between the range of concentrations and the mean value.

For most elements, the median of the coefficients of variation obtained for concentrations in solutions collected at different pressures, exceeded that of the relative difference of repetitive measurements. For elements with an average concentration above 1 µg/L this is the particularly the case for Ni, Mn, Fe, Mo, Cu, Zn, Rb, Co, Cs, As, Sb, V and U. This suggests, that the variability related to increasing

the pressures considerably exceeds that of analytical errors. An increase in variability can originate from systematic effects, reflecting pressure dependency on the composition of solution. Alternatively, the increase in variability can also be caused by erratic effects including contamination.

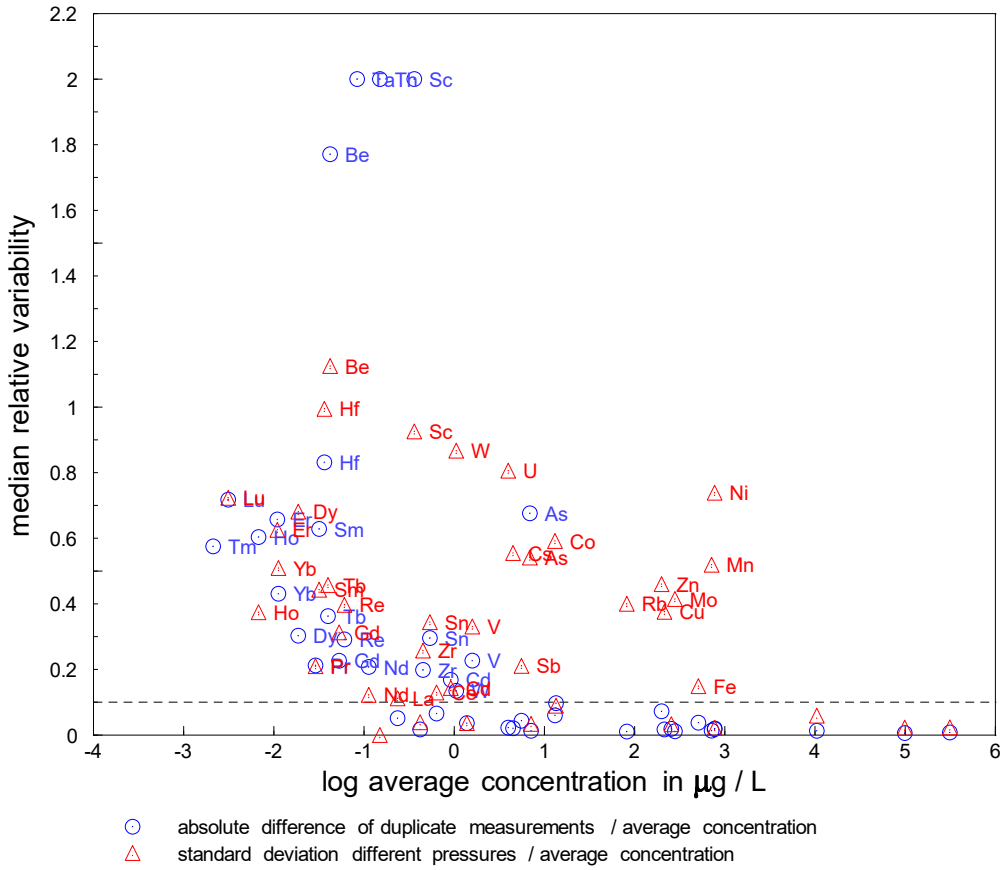

Fig. 9 Comparison of relative variability for replicate measurements and application of different pressures during squeezing as a function of the average concentration of the respective elements. For replicate measurements, the absolute difference of two measurements was normalized to the corresponding mean value. In view of the effect of pressure, the standard deviation of concentrations measured in solutions obtained upon increasing the pressure was normalized to the corresponding average concentrations. The figure shows the median relative variabilities for all samples as a function of the logarithm of the average concentrations over all samples and replicates. Elements, for which the median of the difference between measurements or of the coefficient of variation for solutions obtained at different pressures was larger than 10 % (ratio 0.1), the name is plotted as a label in the respective colours.

In order to evaluate possible changes in trace element composition upon contact with the materials of the pressure cell and connected tubing, a test solution was passed through the cell and tubing. One sample was passed through the squeezing cell, the stainless steel filter and the outgoing tubing. The second solution was remaining test

solution in the squeezing cell, which has been in contact with the cell and the filter. The test solution was an internal reference seawater sample collected in the Mediterranean Sea. This test solution has not been subjected to trace element analyses so far. It turned out that concentrations of most trace elements by far exceeded those reported for pristine open ocean water (Sohrin and Bruland, 2011 and references therein). This limited the sensitivity of the test towards possible contamination as a release of elements into the test solution upon contact with the squeezing cell and tubing could only be detected when the contamination resulted in a significant increase of the concentration of the corresponding element.

Upon contact with the device, the largest relative increases in concentration, with a factor larger than 10, was observed for the elements Cu, Zr, Sn and Hf (Fig. 9). For these elements, the enrichment resulted in concentrations in the range observed in waters retrieved from the clay samples when taking the concentrations in seawater as a reference. Hence, for these elements, contamination of the collected solution upon contact with the pressure cell and tubing produces unreliable values for the in situ porewater.

However, there are also indications that the concentrations of other elements are affected by to release of removal of these elements upon contact with the pressure cell or tubing. It might be possible, that the sorption or release of some elements requires elevated pressure or longer residence time in comparison to the conditions applied for flushing of the cell with seawater. This is the case for all elements, for which the variability, related to different pressure application, exceeds that of analytical error and there are no indications for systematic pressure dependency on measured concentrations. This conclusion is based on the assumption that squeezing artefacts lead to random error. Increasing the squeezing pressure did not generate consistent concentration trends across elements (Fig. 11). For cores C20 and C57, element concentrations remained relatively stable across the 5 - 50 MPa pressure range, with most elements clustering within ±1 log unit across all pressures. The lanthanide region (shaded area) similarly showed no systematic pressure dependence for these cores. Core C75 represented a partial exception, showing somewhat greater variance between pressure steps but changes did not follow a consistent increasing or decreasing pattern with pressure.

The absence of a clearly identifiable systematic effect of pressure on concentrations in the corresponding solutions implies that, for all above listed elements with an average concentration above 1 µg/L including Ni, Mn, Fe, Mo, Cu, Zn, Rb, Co, Cs, As, Sb, V and U, alteration in concentration due to squeezing artefacts should be considered as a possibility. In particular, measured concentrations for Ni very unlikely reflect concentrations of the in situ porewater. Measured concentrations in the squeezed solutions range between 150 and 2200 µg/L while typical concentrations in natural waters are in the range of a few µg/L and only exceptionally exceed 100 µg/L.

High Ni concentrations could be caused by release from steel or erosion of nanosized steel particles and their, possibly only partial, dissolution upon the acidification of the sample. Next to Fe and C, Cr, Ni, Mo and Mn are, in decreasing order of weight percentage, components of the alloy used to construct the pressure cell (see appendix). The deviating concentration pattern of trace elements in the sample from C62 can be attributed to the dissolution of steel particles. That is because the deviation is most pronounced for the elements Fe, Ni, Cr, and to a lesser extent for Mo, the main components of the steel. This implies that the enrichment in lanthanides in this sample, possibly present as traces in the steel, might also be attributed to the contamination of the retrieved solution from core C62 with steel particles. In contrast to the sample from core C62, high concentrations in Ni were not accompanied by proportionally elevated concentrations in Cr in samples from other cores. This indicates that elevated Ni concentrations cannot be solely ascribed to contamination with steel particles. Hence, in case that elevated Ni concentrations in the retrieved solutions are a contamination artefact, selective release from the steel could provide an explanation.

In general, the plausibility of measurements of elements exhibiting significantly larger concentrations in the squeezed pore water compared to the seawater used in the preliminary tests should be critically assessed. For other elements, possible contamination could not be excluded due to the limitations of the test. That is, the concentration in the squeezed solutions did not significantly exceed the initial concentrations in the test solution, possibly masking contamination during the test.

In Fig. 10, the elemental concentrations in the measured solutions were normalized to the corresponding concentrations in the seawater, used in the preliminary tests. In comparison to this seawater, the collected water from the clay samples was consistently, relatively enriched by more than a factor of 10 for the elements Mn, Co, Ni, Sr and Ba (ignoring Sn due to the ascertained origin from contamination). Highest relative enrichment was found for Cs but the relative enrichment was very variable with an enrichment factor spanning almost four orders of magnitude. The water of most samples was enriched with the lanthanides between La to Eu. For the lanthanides in the series Gd – Yb the trend is inconsistent with samples relatively enriched and others depleted. In the following, natural processes possibly accounting for the consistently, largest relative enrichment of Mn, Co, Ni, Sr and Ba will be discussed.

The release of Ni and Co upon oxidation of pyrite could account for their mobilization and has been described for Ni (Larsen & Postma, 1997). However, pyrite oxidation requires the intrusion of potential oxidants, such as O_2 or NO_3 into the clay layers. Although oxidation artefacts upon collection and handling of the cores cannot be completely excluded, there are no other indications for pronounced pyrite oxidation such as elevated SO_4 concentrations or decrease in pH and alkalinity due to the related acidification. On the contrary, SO_4 concentrations in the collected solutions are with values between around 0.1 and 0.5 mM (see appendix) much lower compared to seawater (around 28 mM). Depletion of SO_4 is likely caused by microbial sulfate reduction in the subsurface, and groundwater adjacent to the investigated formations possibly might be already depleted in SO_4. Consumption of SO_4 can drive release of Ba from barite, and has been proposed as a reason for elevated Ba concentrations in groundwaters (Moore & Staubitz, 1984). Usually Fe concentrations exceed those of Mn due to the larger abundance of Fe in earth materials, with the exception of a view environments, specifically enriched in Mn. The latter include redox clines in anoxic basins. Abrupt oxidation events, for example, can result in the sedimentation of large amounts of Mn (oxyhydr)oxides transforming into $MnCO_3$ (rhodochrosite) upon diagenetic processes (Lenz et al. 2014). Dissolution of $MnCO_3$ can be a source for Mn enrichment of porewaters. For comparison, the equilibrium concentrations with an alkalinity of 2 mEq, pH 7.8. I = 0.5 M and T = 10°C (as an approximation to the measured values in the solutions) is about 1800 µg/L and hence, exceeds, the

measured Mn concentrations of almost all solutions. Finally, Sr concentrations are highest for all elements analysed by ICP-MS and also show a high enrichment in the solutions compared to seawater. High Sr concentrations in groundwaters are generally ascribed to the dissolution of carbonates or the transformation of Sr-containing aragonite into Sr-poor calcite. The measured concentrations are higher in comparison to those reported for freshwater systems (Musgrove, 2021) and also exceed values expected in equilibrium with strontianite $SrCO_3$ (around 46,000 µg/L calculated for an alkalinity of 2 mEq, pH 7.8. I = 0.5 M and T = 10°C to obtain an indication) by up to about a factor of eight.

In conclusion, a plausible explanation can be given for the enrichment of the porewaters in Ba, Sr and Mn, while elevated concentrations for Sr are possibly a consequence of applying a high pressure during squeezing. However, for the enrichment in Co and Ni no plausible explanation can be found, implying that the relatively high concentrations of Co and Ni are likely caused by contamination. In any case, pronounced enrichment in the porewater due to transformation of dissolution of mineral phases should also be reflected in the other applied techniques, in particular aqueous extractions, and the discussion will be continued in the corresponding sections.

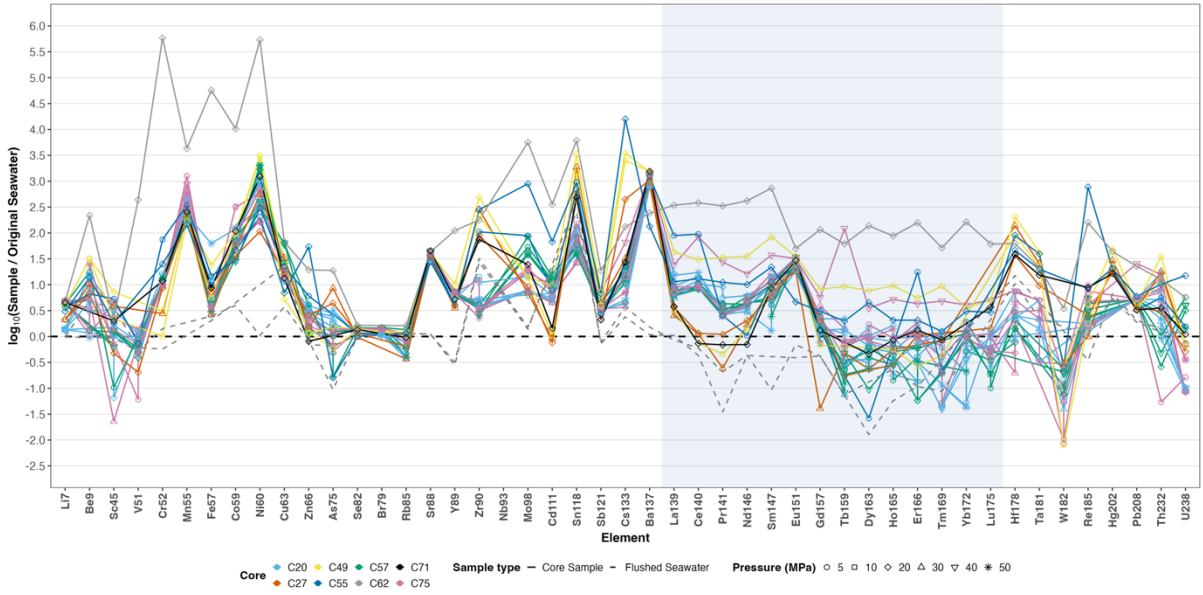

Fig. 10 Comparison of squeezed porewater composition relative to seawater used in preliminary contamination tests (log_{10} concentration ratios normalized to seawater). Values above the dashed zero reference line indicate enrichment relative to the seawater used to flush the squeezer, while values below indicate lower concentrations. The dashed lines reflect the composition of the seawater collected after

flushing the squeezing cell. The shaded area highlights rare earth elements (REEs). Each coloured line represents a different core (C20, C57, C75) with symbols indicating applied pressure (5-50 MPa).

Fig. 11 Pressure-dependent trace element patterns in squeezed porewater by formation (log_{10} concentration ratios normalized to seawater). Top panel: C20, middle panel: C57, bottom panel: C75. Each colored line represents a different applied pressure (5, 20, 30, 40, 50 MPa). The shaded area highlights rare earth elements (REEs). Comparison across panels reveals formation-specific responses to applied pressure during squeezing. Note, the reported Se concentrations are not reliable due to spectral interferences (see appendix)

3.3 Aqueous extraction

Aqueous extraction experiments were conducted on replicate subsamples from cores C20, C57, and C75 using systematic variations in solid:liquid ratio (25 g/L and 200 g/L), extraction solution (DI water and 0.1 M $NaHCO_3$), and extraction time (1, 7, and 28 days).

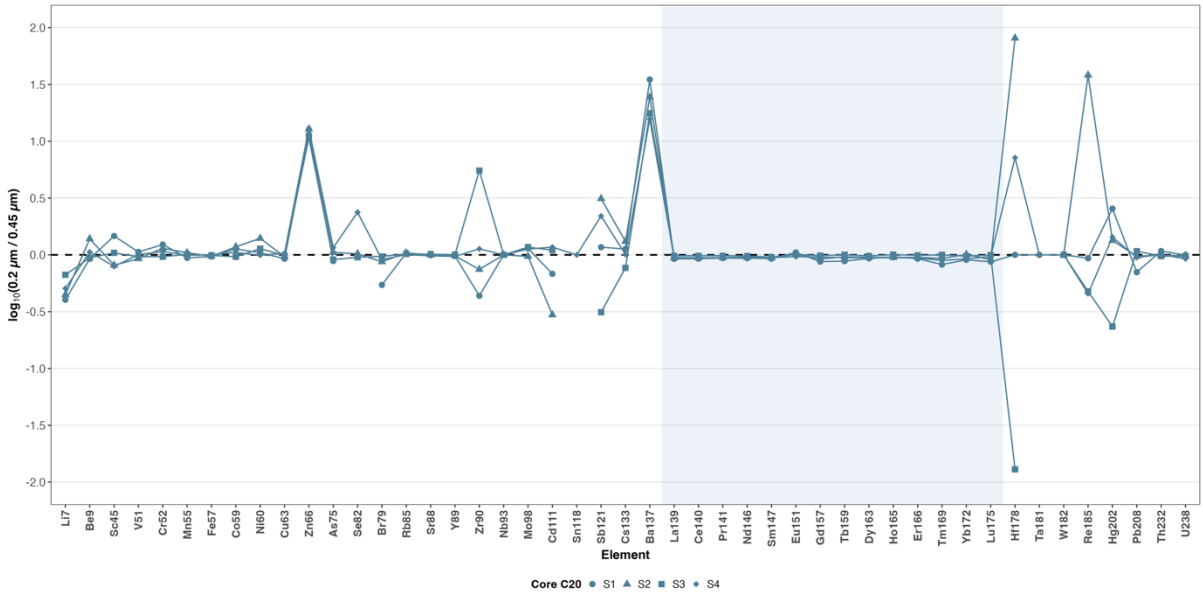

Fig. 12 Effect of filtration on trace element concentrations in aqueous extraction experiments (log_{10} concentration ratios of 0.45 µm to 0.2 µm filtered samples). Core C20 was extracted with deionized water at solid:liquid ratios of 25 g/L and 200 g/L. Values below the dashed zero reference line indicate higher concentrations in 0.45 µm filtered samples compared to 0.2 µm filtered samples, suggesting presence of colloidal material between 0.2-0.45 µm size range. The shaded area highlights rare earth elements (REEs).

Sequential filtration through 0.45 µm and 0.2 µm membranes was tested on core C20 extracts to evaluate colloidal contributions in the size range between 200 and 450 nm. The ratios of concentrations measured after each filtration step are presented in Fig. 12 in log_{10} scale. Most elements cluster around the zero reference line, reflecting a concentration ratio of 1 and, hence, no change in concentration upon filtration with a filter of a pore size of 0.2 µm. For most elements, log_{10} ratios were between -0.5 and +0.5, indicating that filtration through 0.45 µm versus 0.2 µm produced minor differences for the majority of trace elements. This suggests limited presence of colloidal material in the 0.2-0.45 µm size range, or that colloids in this size range do not carry significant trace element loads.

Notable exceptions include sharp positive spikes (log_{10} ratios >1.0) for Zn, Ba, and Hf in all samples. For these elements, concentrations after 0.2 µm filtration were more than 10 times larger than after 0.45 µm filtration. That is, the solutions became contaminated in these elements after the first filtration step. For Hf, the test is of lower informative value as, in many measurements, concentrations were below detection limit and small absolute deviations result in large relative effects. For Zn and Ba, the source of the contamination in this set of samples remains enigmatic. This is also

because the contamination is specifically pronounced for these two elements. Contamination upon the 0.2 µm filtration itself, is unlikely as for other samples lower Zn and Ba concentrations were obtained in 0.2 µm filtrates as those in the 0.45 µm filtrates in the test.

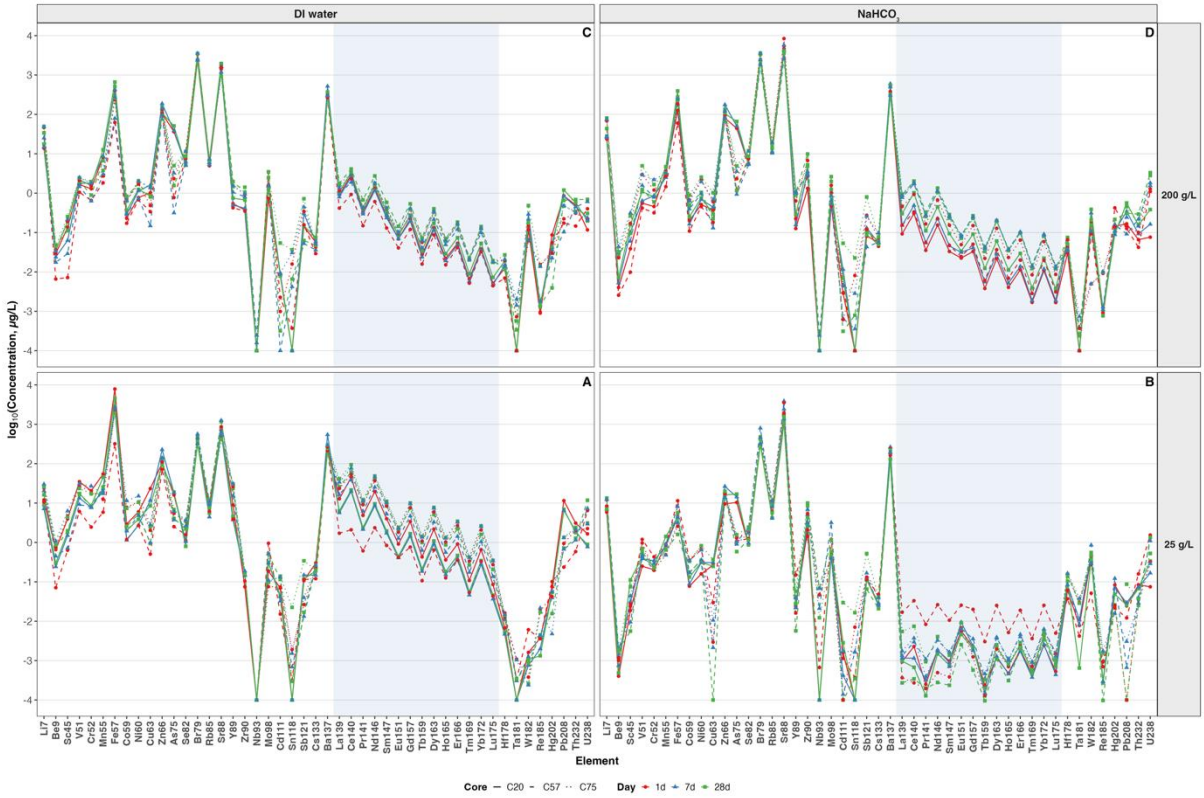

Fig. 13 Effect of extraction time (coloured lines) on trace element concentrations in aqueous extraction experiments (A and B: DI water(A) and $NaHCO_3$(B) extraction at 25 g/L, C and D: DI water(C) and $NaHCO_3$(D) extraction at 200 g/L in log_{10} scale, µg/L). Left panel: deionized water extraction; right panel: 0.1 M $NaHCO_3$ extraction. Each point represents average concentration of duplicate measurements. Different line type represents different core with colours indicating contact time (1d, 7d, 28d). The shaded area highlights lanthanides. Note, the reported Se concentrations are not reliable due to spectral interferences (see appendix)

Figure 13 provides an overview of all results from aqueous extractions of material from all cores including different solid: liquid ratios, duration of extraction, presence or absence of bicarbonate. On a first glance, the patterns of elemental concentrations were similar for the same solid:liquid ratio and the same extraction solution. That is, extraction time and extracting material from different cores and from different layers within one core only resulted in relatively little variability in concentration patterns. The effect of extraction time will be analysed in more detail below.

Despite the conformity of elemental concentration patterns within each of the four groups presented in Fig. 13, there are obvious inconsistencies when comparing the concentrations for different solid:liquid ratios or, for cross-validation, comparing the concentrations in aqueous extracts and those in the solutions obtained from high pressure squeezing. These inconsistencies, discussed in the following, constrain not only the reconstruction of porewater composition using aqueous extractions but also the possibilities for evaluating the effect of bicarbonate addition to the extraction solutions.

Systematic variation of solid:liquid ratios allows to determine the porewater concentrations of (virtually) inert solutes when plotting the corresponding reciprocal concentrations (1/C) against the ratio between the added volume of water for the extraction (V_{added}) and the mass of extracted sediment (m_{solid}) (Behrends et al., 2016):

$$\frac{1}{C} = \frac{V_{pore}}{n_{pore}} + \frac{m_{solid}}{n_{pore}} * \frac{V_{added}}{m_{solid}}$$

The intercept of the regression line is the reciprocal porewater concentration: the ratio between the number of moles of the solute in the porewater (n_{pore}) and the pore volume (V_{pore}). With only two solid:liquid ratios, the systematic uncertainty of the value of the intercept is large due to the required extrapolation. However, as the pore volume per mass of sediment has been independently determined, porewater concentrations can be deduced when dividing the ratio m_{solid}/V_{pore} with the calculated slope (m_{solid}/n_{pore}).

For inert solutes, the duration of the extraction is not expected to be relevant as, per definition, no reactions with the solid phase are taken into consideration and also absence or presence of bicarbonate should have no effect. Hence, for inert solutes, the average concentrations over different extraction times and the two different extraction solutions can be used.

Table. 3 Bromine concentrations measured in solutions obtained from high-pressure squeezing using ICP-MS (value over all pressures and duplicate analyses), ICP-OES (see appendix) and calculated based on aqueous extractions in mg/L.

Core	Squeezing ICP-MS (n = 8 to 10)	Squeezing ICP-OES (n = 2)	Aqueous extraction (n =4)
C20	83 ± 1	89-96	58 ± 1
C57	111 ± 2	120-125	89 ± 13
C75	106 ± 3	112-117	68 ± 13

The results of applying this approach to obtain Br concentrations in porewater are presented in Tab. 3 for the three cores. The values obtained for the four samples from one core had an coefficient of variation of below 20 % but were systematically lower, up to 35 %, compared to the values obtained from high-pressure squeezing based on ICP-MS measurements. The systematic difference is not unexpected and can be explained by anion exclusion due to electrostatic effects. That is, solution obtained from high-pressure squeezing originates predominately from larger pores not affected by anion inclusion. In contrast, aqueous extractions upon suspension also includes anion-depleted solution from smaller pores (Behrends et al. 2016). This example demonstrates the expedience of this approach and support the assumption that Br concentrations in the extracts are a consequence of the dilution of porewater and to a lesser extent affected by reactions with the solid phase.

In contrast to Br, decreasing concentrations of other solutes in the aqueous phase upon dilution can trigger the release from the solid phase in order to re-establish equilibrium or steady state. When the porewater concentration of an element is controlled by thermodynamic equilibrium with the solid phase and reaction kinetics are fast enough to reach equilibrium during extraction time, the measured concentration in the extract can represent the concentration in the porewater. This is the case if the corresponding reactive solid phase is present in excess or, in general, consumption of the part of the solid-bound pool does not change the chemical potential of the element in the solid phase. For example, this would be the case if desorption of ions from the sorption complex, as a response to the dilution of the aqueous solution, does not significantly change the relative occupation of surface sites among the different ions.

If these requirements are fulfilled, the solid:liquid ratio does not affect the concentration of the element in the extract. The situation is more complex in case of minerals, for which the ratio of dissolved ion concentrations in the porewater, in equilibrium, significantly deviates from the stoichiometric ratio in the mineral. Typical examples are sulphides. In environments with elevated dissolved sulphide concentrations, concentrations of chalcophile metals can be reduced to trace levels due to the low solubility of the corresponding sulphides. Re-establishing equilibrium via congruent dissolution of sulphides upon dilution of the porewater would than lead to higher metal concentrations than in the original porewater.

In the case that reactions with the solid phase release elements into the solution but equilibrium or steady state is not reached during the extraction, concentrations in the extract at high solid:liquid ratios are expected to be higher than in extracts at low solid:liquid ratio, and higher than expected based on the lower dilution factor, alone. In these cases, monitoring the time evolution of concentrations and the effect of bicarbonate (for example if dissolution of carbonates play a role) can provide complementary information on the relevance and nature of these reactions.

These conceptual consideration create a framework to assess the consistency of the measured concentrations and cross validation with results obtained with other approaches. Specifically, the ratio in concentrations obtained for the different solid:liquid ratios should be in the range between 1 and the ratio in dilution factor related to the aqueous extraction (about eight times higher concentrations in the 200 g/L extracts compare to 25 g/L extracts). In view of comparison with solutions from high-pressure squeezing: concentrations in extracts should, in general, not be higher compared to those in squeezed solutions. On the opposite, concentrations in aqueous solution can be lower than in the squeezed solutions, but not beyond the factor expected from porewater dilution. That is, Br normalized concentrations should not be higher in squeezed solutions compared to aqueous extracts.

To assess whether extraction time produced a systematic effect on trace element concentrations, a two-step sign test was applied using all three time points (1d, 7d, 28d). For each subsample, the direction of change from 1d to 7d and from 7d to 28d was classified as either concordant (both steps in the same direction, indicating a

monotonic trend) or discordant (steps in opposite directions, indicating oscillation). Comparisons were pooled across all cores, solid:liquid ratios, and extraction solutions (n = 48 per element) and tested with a two-sided binomial test. For 30 out of 47 elements, discordant pairs dominated ($p \geq 0.05$), indicating that concentrations oscillated between time points rather than changing monotonically (Fig. 14). This confirms that for the majority of elements, no systematic time-dependent trend exists, and concentration variability between time points reflects analytical and spatial scatter rather than kinetic evolution. For 17 elements (V, Cr, Fe, Zn, Rb, Sn, Cs, Ba, Gd, Tb, Dy, Er, Tm, Lu, Ta, W, Br), significantly discordant behavior was detected ($p < 0.05$), suggesting a consistent oscillation pattern for these specific elements. However, this implies that for none of the elements, a consistent increase in concentration with extraction time was observed, which would be expected from a continuously proceeding release from the solid phase.

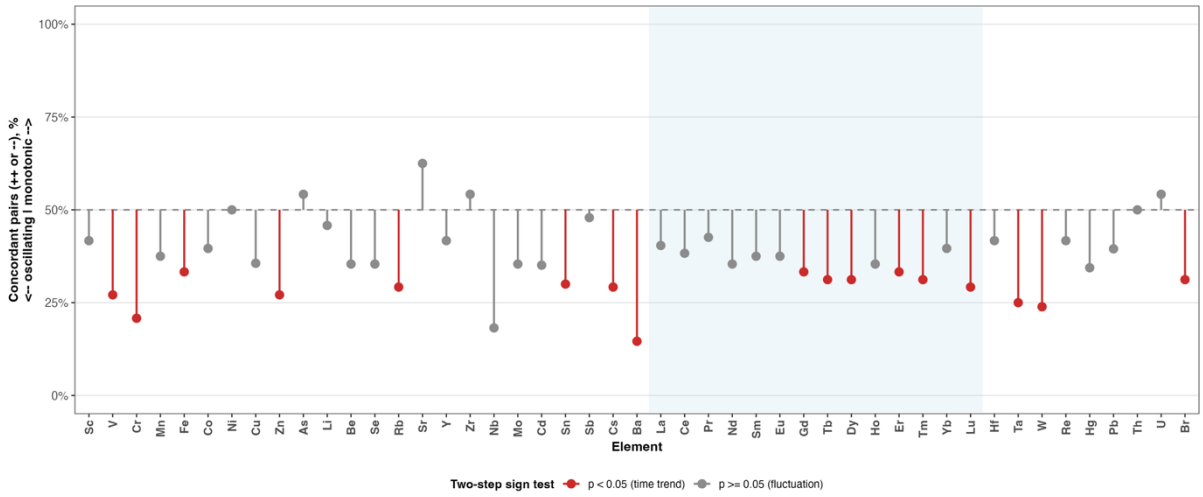

Fig. 14 Two-step sign test results for the effect of extraction time on trace element concentrations in aqueous extractions. The y-axis shows the percentage of concordant pairs (both consecutive time steps 1d→7d and 7d→28d changing in the same direction) out of 48 pooled comparisons per element. The dashed line at 50% represents random fluctuation with no directional preference. Values below 50% indicate oscillating behavior (discordant pairs dominate). Red symbols indicate elements where the deviation from 50% is statistically significant ($p < 0.05$, two-sided binomial test).

Comparison of concentrations for the two different solid:liquid ratios reveals contradictions with the expected trends. More specifically, for several elements, including lanthanides as well as Fe, Co, Ni, Mn, Cr, V, Sc and U, concentrations obtained with DI water and a solid:liquid ratio of 25 g/L exceeded those for the 200 g/L extracts (Fig. 15). Furthermore, Fe concentrations in the 25 g/L DI water extracts were

more than 10 times larger compared to the concentrations in the solutions obtained from high pressure squeezing. Higher Fe concentrations could be explained by the dissolution of Fe phases such as siderite $FeCO_3$ or FeS due to the dilution of dissolved inorganic carbon or sulphide when extracting with DI water. However, this cannot explain the considerably higher concentrations at low solid:liquid ratio compared to the 200 g/L extracts. More likely, the high Fe concentrations in the aqueous extracts are caused by the presence of colloidal, Fe-rich particles, which have passed the 0.2 μm filters. Other elements with elevated concentrations in the 25 g/L extracts are presumably associated with these Fe-rich colloids.

In contrast to DI water extracts, concentrations in the 200 g/L extracts with 0.1 HCO_3 were for most elements and samples higher compared to those in the 25 g/L extracts. However, for Fe and, particularly, lanthanides the concentration difference for samples C75 and C20 by far exceeded the factor of 8, which could be attributed to different dilution of the pore water. For Fe, concentrations in the 25 g/L were more than a factor of 70 smaller. Although other explanation could be given, the larger than expected discrepancy in concentrations of Fe, lanthanites and some other elements for the different solid:liquid ratio can also be attributed to higher abundance of Fe-rich colloids in the 200 g/L extracts compared to the 25 g/L extracts. However, it remains enigmatic why the contribution of colloids appears to be systematic within one group of extractants with respect to the addition of DI water or HCO_3 solution and the solid:liquid ratio.

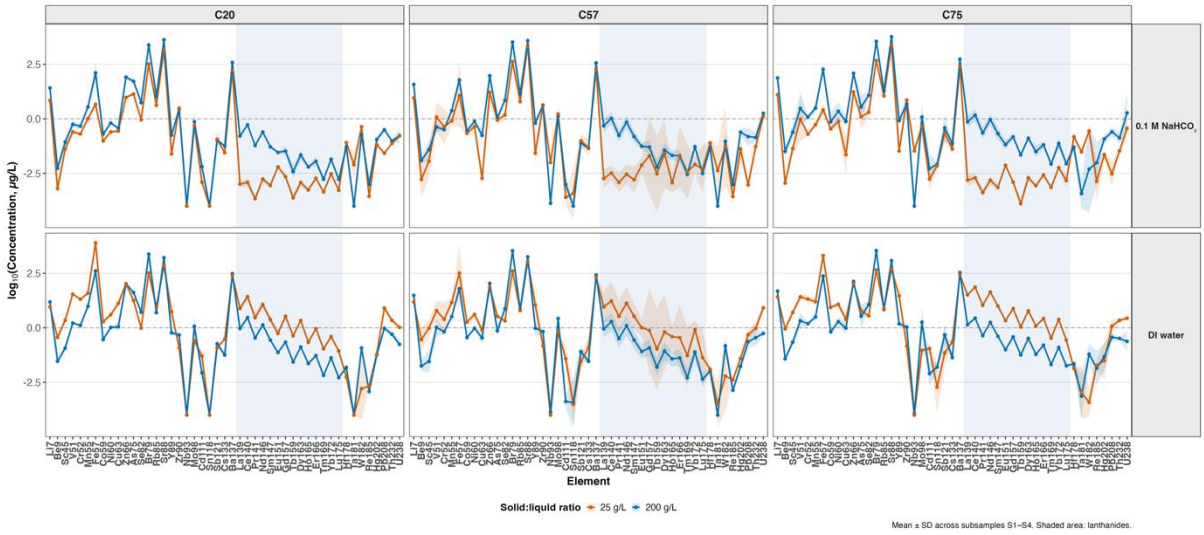

Fig. 15. Effect of solid:liquid ratio on trace element concentrations in aqueous extractions. Mean ± SD of log_{10} concentrations across subsamples S1–S4 for 25 g/L (orange) and 200 g/L (blue) solid:liquid

ratios, shown for each core (C20, C57, C75; columns) and extraction solution (0.1 M $NaHCO_3$, top; DI water, bottom). Shaded ribbons indicate ±1 SD. Elements without a systematic time trend (n = 30) are represented by the mean of 1d, 7d, and 28d extractions; elements with a systematic time trend (n = 17) are represented by 1d extraction only. Note, the reported Se concentrations are not reliable due to spectral interferences (see appendix)

Although, the concentration of dissolved trace elements in the aqueous extracts might be overestimated due to the presence of colloids, the obtained values provide an upper limit for Br normalized concentrations, which should not be exceeded in the solutions obtained from high-pressure squeezing. For Ni and Sr, the median of the value for squeezed solutions is located above the upper quartile of the log of ratios obtained in the aqueous solutions. These relatively high Ni/Br ratios in the squeezed solution support the conclusion that Ni concentrations in the squeezed solutions were enhanced due to contamination. The relatively high Sr/Br ratios suggest that also Sr release was enhanced due to applying a high pressure.

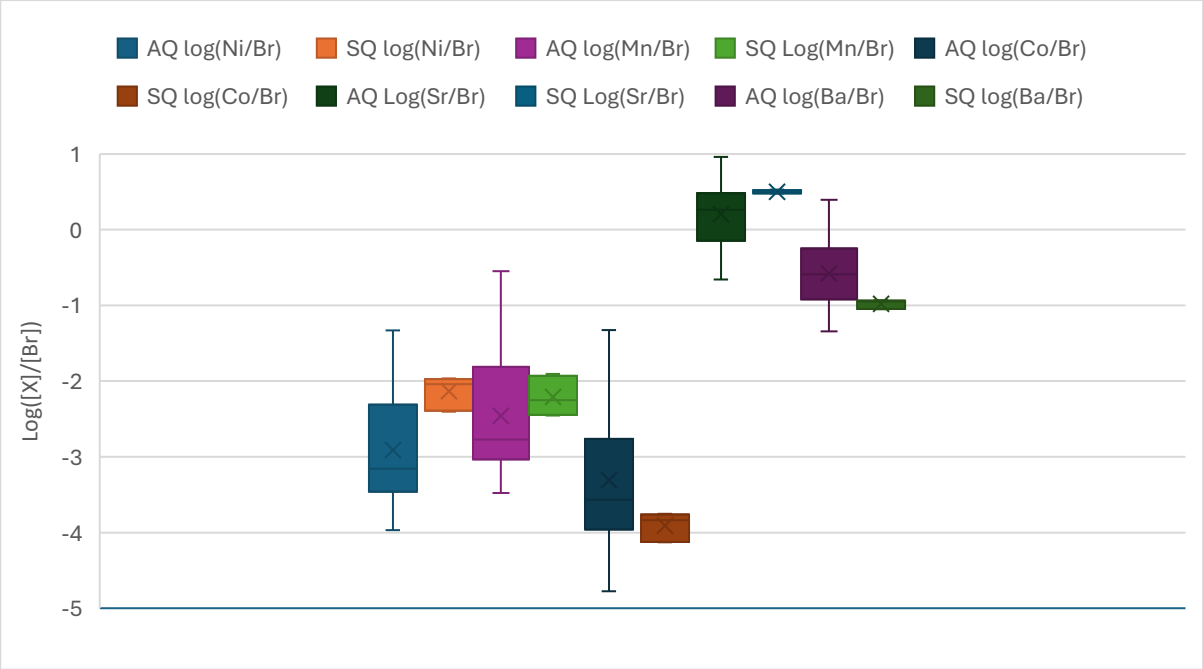

Fig. 16. Box plots of the $\log_{10}$ of Br normalized concentrations of selected elements for comparing the ratios obtained in aqueous extractions (AQ) and those in solutions obtained by high-pressure squeezing (SQ).

3.4 Paper absorption

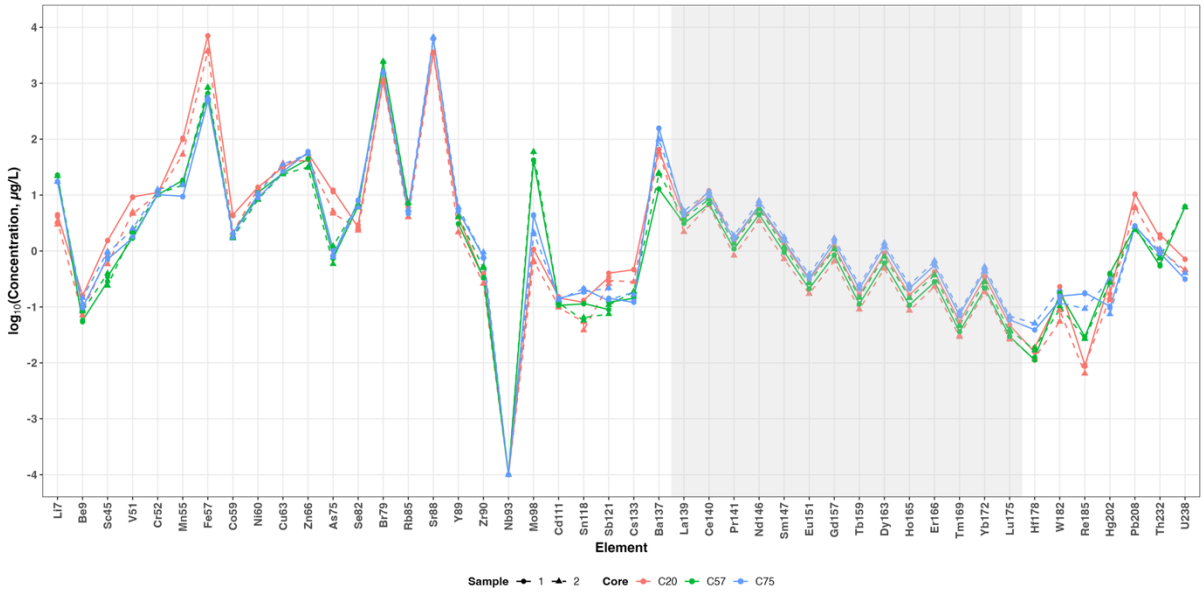

Fig. 17 Trace element concentrations in porewater extracted by paper absorption method (log_{10} scale, µg/L). Two replicate samples were tested from each core:. Samples were equilibrated for two months with cellulose filter paper inserted between split core halves. The shaded area highlights rare earth elements (REEs). Solid and dashed lines distinguish between replicates (samples 1 and 2) from each core. Note, the reported Se concentrations are not reliable due to spectral interferences (see appendix)

Trace element concentrations obtained from paper absorption (Fig. 17) show consistent concentration patterns among cores and replicate samples. Concentrations span approximately six orders of magnitude, from below detection limits to >10^4 µg/L. Most elements display log_{10} concentration (in µg/L) ranging from -1 to +2, with several notable exceptions showing elevated concentrations (Fe, Br, Sr, Mo and Ba). The lanthanides (shaded region) exhibit concentrations ranging from below detection limit to approximately 10 µg/L (log_{10} ~+1).

Visual examination of papers after the two-month contact period revealed minimal water absorption, with papers remaining apparently largely dry. Due to the limited water transfer it was not possible to accurately determine the actual volume of porewater absorbed by the paper via weighing. Secondly, absorption of very small volumes increases the sensitivity to extraction artefacts as some clay particles adhered to filter papers, which can released trace elements upon leaching the papers with acid solution.

However, based on results from aqueous extractions, Br behaves virtually conservatively in the porewater of the sediments. Furthermore, it can be assumed that Br predominately occurs in dissolved form in the samples. Hence, normalization to Br concentrations can open the possibility to reconstruct the composition of the absorbed porewater but also to validate the results from paper absorption by comparing it with the corresponding concentration ratios in squeezed porewater.

Only for a few elements, the Br normalized concentrations in solutions from high pressure squeezing were higher compared to those from extracting the filter papers (Fig. 18). This was consistently the case for Ba and, in sample C57 for Ni, in sample C75 for Mn, and in sample C20 for Mo. For a few other elements, the ratios were very similar. This was particularly the case for Sr and Li. For most elements, the ratios were larger, with up to more than three orders of magnitude for most lanthanides, obtained from paper absorption compared to solutions obtained from squeezing. One prominent example of elements with a concentration above 1 µg/L in squeezed porewater and up to about 1000 times larger Br normalized concentrations based on paper absorption, is Fe. The relatively higher abundance of Fe in the paper extracts can be explained by the release from solid particles, adhering to the filter paper when retrieved from the cores. This implies that also the higher abundance of other elements in the filter extracts is likely caused by the release from adhering clay particles during the acid extraction of the filter papers. Hence, an attempt was made to correct for the particle-bound contribution to the paper extracts by correcting the Br normalized concentrations based on the excess abundance of Fe compared to squeezed solution and the Fe normalized contents in the solid phase reported by Hoving et al. (2025).

Using the excessive abundance of Fe in the paper extracts in order to correct for the solid-phase derived contribution to the extracts did not significantly improve the consistency between data from squeezed solutions and paper absorption(Fig. 19). In some cases, such as for Hf or Zr, the correction resulted in negative concentrations, which are presented as Br normalized ratios of zero in Fig. 19. The position of most elements moved towards the 1:1 line in Fig. 19 upon the correction, but the Br normalized concentrations remained orders of magnitude larger compared to those in the squeezed solutions. This can be explained by preferential release of these elements from the solid phase during acid extraction of the filters compared to Fe. This

could be, for example, the case when the relative occupation of the sorption complex by these elements is larger compared to Fe and acid extraction induced predominately desorption and to a low extent dissolution of Fe-rich silicates.

Despite these limitations, the results from the paper absorption experiments can contribute to the cross-validation of the measured concentrations from high pressure squeezing. Similar Br normalized concentrations in the paper extracts and squeezed solutions, enhance the confidence in the measured concentrations of Li, and Sr in the squeezed solutions. The consistently higher values for Ba in the squeezed solutions suggest that the release of Ba to the porewater was enhanced when applying high pressure. Indications for the suspected contamination of squeezed porewater with Ni and possibly Co from paper absorption are not strong. Ni/Br ratios in the squeezed porewater are only higher in sample C57. That is, for the other samples, elevated Ni/Br ratios in the paper extracts due to release from solid particles during the paper extraction could mask the contrast with squeezed porewaters affected by Ni contamination.

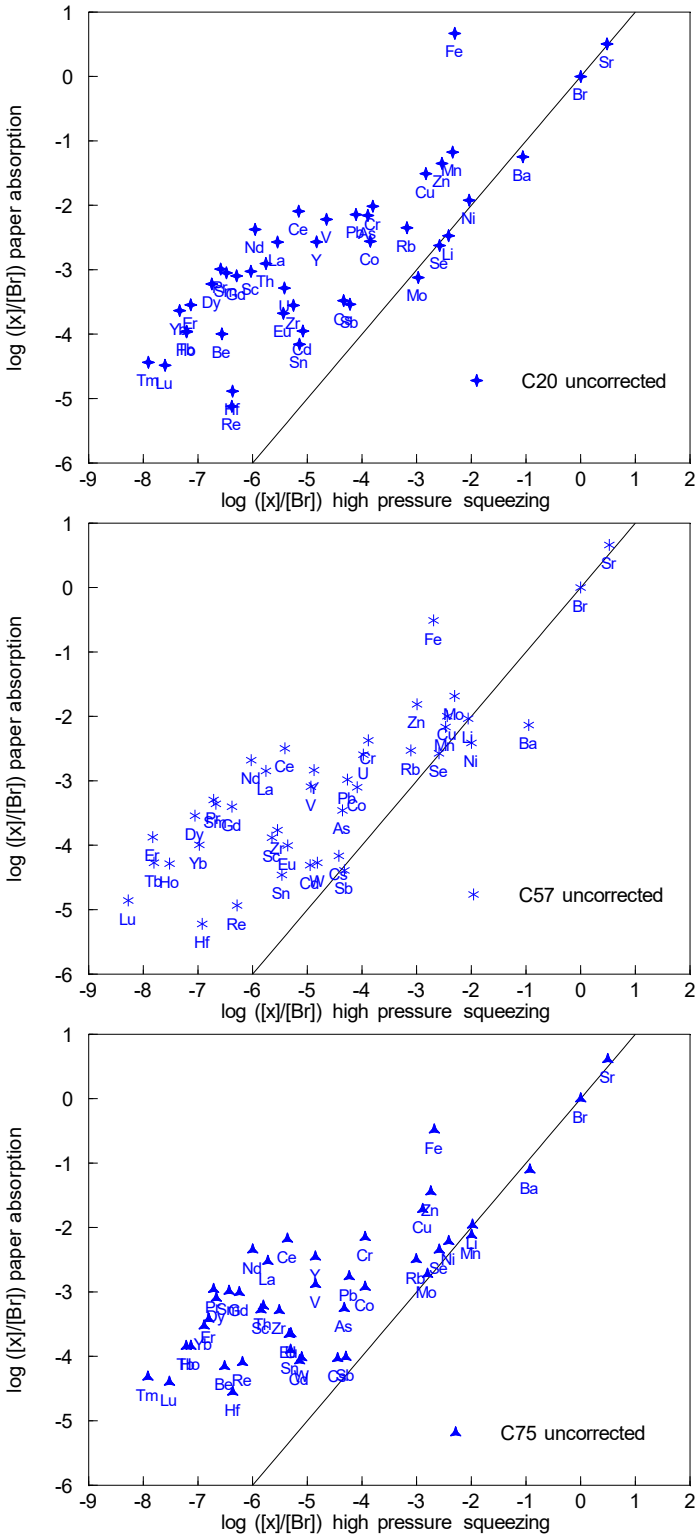

Fig. 18 Average, bromine normalized, elemental concentrations of acidic extracts from filter papers after two months contact time with the clay sediments as a function of the corresponding ratios in solutions obtained from high pressure squeezing of the same cores. The ratios are presented in log scale and the black line indicates the 1:1 ratio. Note, the strong agreement of Se/Br ratios for both methods is an analytical artefact due to spectral interference (see appendix).

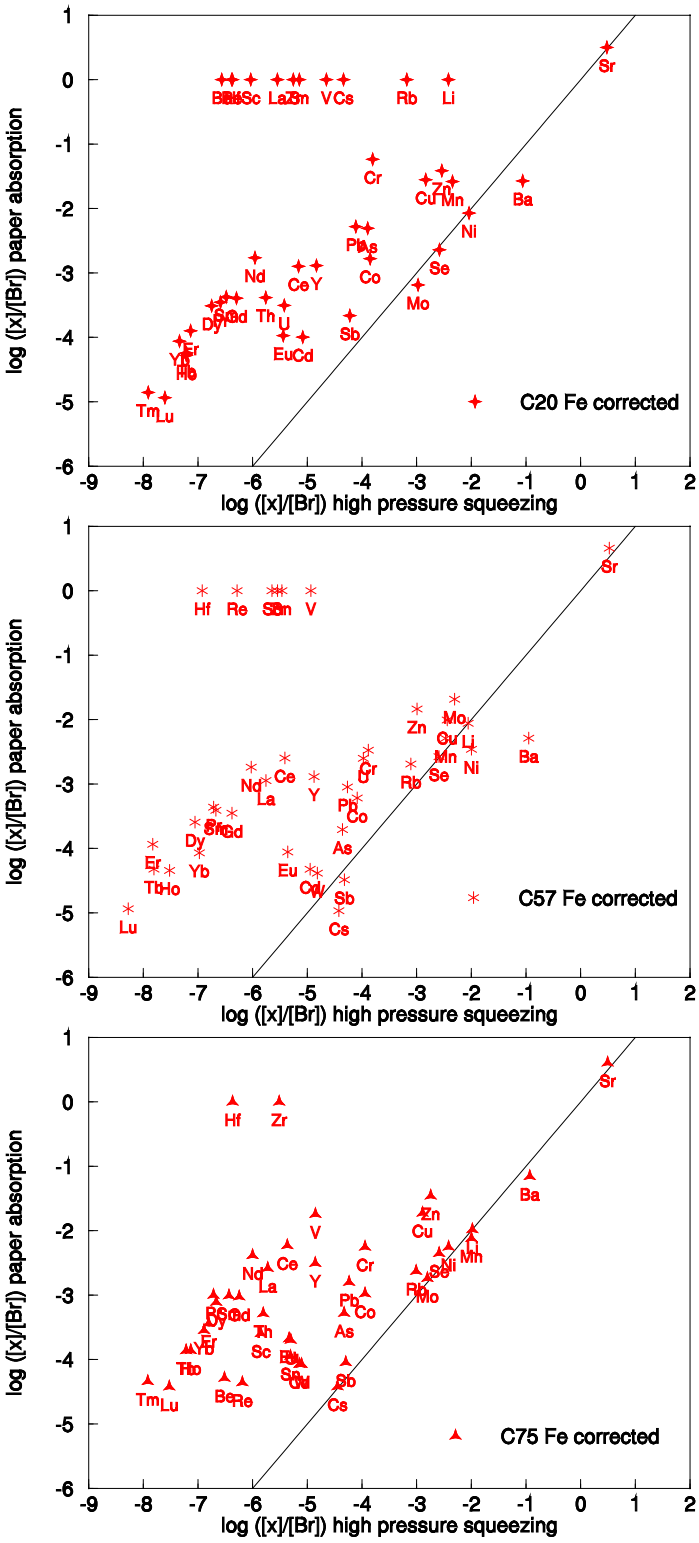

Fig. 19 Average, bromine normalized, elemental concentrations of acidic extracts from filter papers after two months contact time with the clay sediments as a function of the corresponding ratios in solutions obtained from high pressure squeezing of the same cores. The ratios for the acidic extracts were corrected based on the excessive abundance of Fe and the Fe normalized contents in the corresponding solid phase of the clay samples. When the correction led to negative concentrations, the results are presented with a value of zero for the paper absorption ratios. The ratios are presented in log

scale and the black line indicates the 1:1 ratio. Note, the strong agreement of Se/Br ratios for both methods is an analytical artefact due to spectral interference (see appendix).

4. Conclusion

This systematic comparison of porewater extraction methods applied to Dutch Paleogene and Neogene clay formations reveals that measured trace element concentrations depend critically on sampling technique, with method-specific artifacts leading to concentration changes by 1–4 orders of magnitude across the element suite. It turned out that validation of the measured concentrations is challenging.

High-pressure squeezing can be potentially biased from steel contamination, in particular Ni but also Mn, Mo, Cr and Co. Paper absorption and aqueous extractions do not provide representative absolute concentrations for trace elements in the in situ porewater. However, normalization to Br, when assuming conservative behaviour, creates a starting point in the interpretation of the measured concentrations in leachates and extracts. Interpretation of concentrations for trace elements with high affinity to Fe minerals can be additionally complicate the interpretation as the presence of Fe-rich colloids and particles in the extracts and filters (and the corresponding leachates) likely influenced the measured concentrations. However, results from paper absorption and aqueous extraction can add valuable, complimentary information for the interpretation of data from core squeezing and to understand the processes controlling the trace element concentrations in the porewater of clay-rich sediments.

For the interpretation of the measured concentration and to further strengthen the validation, it would be very helpful to sample and analyse groundwater from aquifers adjacent to the clay-rich sediment layers. In order to reduce possible bias in measured trace element concentrations in aqueous extracts due to the presence of Fe-rich colloids, the extracts should be subjected to ultrafiltration prior to analysis. The paper absorption method needs further improvement as the adhesion of clay particles to the filter paper might be an inevitable consequence of establishing close contact between

the filter and the clay sample. Possibly, applying layers of material with decreasing hydraulic potential, i.e. increasing suction force could help to prevent contact between particles and the pore water attracting layers in the interior.

Despite the limitations and remaining uncertainties, this study indicates that the composition of porewaters from the three investigated clay-rich formations are alike. The major ion composition is similar to seawater, but the porewaters are relatively depleted in sulphate. Within the group of elements investigated in this study, the presence of relatively high concentrations of Sr and Ba were supported by all approaches, whereas Sr and Ba concentrations in squeezed porewaters might be increased upon the application of high pressures. For transition elements and elements, which tend to co-occur with Fe in natural environments such as lanthanides or U, no conclusive information on the in situ porewater in the sediment layers can be given due to the likely release or contribution from Fe-rich particles to measured trace element concentrations in aqueous extracts and extracts obtained from filter absorption experiments.

References

Behrends, T., van der Veen, I., Hoving, A., & Griffioen, J. (2016). First assessment of the pore water composition of Rupel Clay in the Netherlands and the characterisation of its reactive solids. *Netherlands Journal of Geosciences*, *95*(3), 315-335.

Bernier, F. (2001). Fracturing and Self-Healing in the Boom Clay: Evidences and Further Studies (No. NEA-RWM-CLAYCLUB--2001-5, pp. 41-45).

Celejewski, M., Barton, D., & Al, T. (2018). Measurement of Cl−: Br− Ratios in the Porewater of Clay-Rich Rocks—A Comparison of the Crush-and-Leach and the Paper-Absorption Methods. *Geofluids*, *2018*(1), 9682042.

Celejewski, M., Scott, L., & Al, T. (2014). An absorption method for extraction and characterization of porewater from low-permeability rocks using cellulosic sheets. Applied geochemistry, 49, 22-30.

Coppin, F., Berger, G., Bauer, A., Castet, S., & Loubet, M. (2002). Sorption of lanthanides on smectite and kaolinite. Chemical Geology, 182(1), 57-68.

De Craen, M., Moors, H., Honty, M., & Van Geet, M. M. (2023). The role of the HADES URL in better understanding of the Boom Clay porewater geochemistry.

De Craen, M., Wang, L., Van Geet, M., Moors, H., 2004. Geochemistry of Boom Clay porewater at the Mol site. Scientific Report SCK•CEN-BLG-990, Mol, Belgium.

Fernández, A. M., & Villar, M. V. (2010). Geochemical behaviour of a bentonite barrier in the laboratory after up to 8 years of heating and hydration. Applied Geochemistry, 25(6), 809-824.

Fernández, A. M., Baeyens, B., Bradbury, M., & Rivas, P. (2004). Analysis of the porewater chemical composition of a Spanish compacted bentonite used in an engineered barrier. Physics and Chemistry of the Earth, Parts A/B/C, 29(1), 105-118.

Gaucher, E. C., Tournassat, C., Pearson, F. J., Blanc, P., Crouzet, C., Lerouge, C., & Altmann, S. (2009). A robust model for pore-water chemistry of clayrock. *Geochimica et Cosmochimica Acta*, *73*(21), 6470-6487.

Hassine, S. B. H., Davies, C., & Garbil, R. (2023). Forty-five years of joint research programmes on geological disposal of radioactive waste and the pioneering role of the HADES Underground Research Laboratory. *Geological Society, London, Special Publications*, *536*(1), 225-236.

Honty, M., Frederickx, L., Wang, L., De Craen, M., Thomas, P., Moors, H., & Jacops, E. (2022). Boom Clay porewater geochemistry at the Mol site: Experimental data as determined by in situ sampling of the piezometers. *Applied Geochemistry*, *136*, 105156.

Hoving, A., Griffioen, J., Kubeneck, J. (2025) Geochemical characterization of Eocene to Miocene deposits of the DAPGEO-2 borehole in Delft, Report TNO 2025 R12729

Kiczka, M., Wersin, P., Mazurek, M., Zwahlen, C., Jenni, A., Mäder, U., & Traber, D. (2023). Porewater composition in clay rocks explored by advective displacement and squeezing experiments. *Applied Geochemistry*, *159*, 105838.

Kim, E., & Boulègue, J. (2003). Chemistry of rhenium as an analogue of technetium: experimental studies of the dissolution of rhenium oxides in aqueous solutions. Radiochimica Acta, 91(4), 211-216.

Lakshtanov, L. Z., & Stipp, S. L. S. (2004). Experimental study of europium (III) coprecipitation with calcite. Geochimica et Cosmochimica Acta, 68(4), 819-827.

Larsen, F., & Postma, D. (1997). Nickel mobilization in a groundwater well field: release by pyrite oxidation and desorption from manganese oxides. *Environmental Science & Technology*, *31*(9), 2589-2595.

Lenz, C., Behrends, T., Jilbert, T., Silveira, M., & Slomp, C. P. (2014). Redox-dependent changes in manganese speciation in Baltic Sea sediments from the Holocene Thermal Maximum: An EXAFS, XANES and LA-ICP-MS study. *Chemical Geology*, *370*, 49-57.

Li, X., Neerdael, B., Raymaekers, D., & Sillen, X. (2023). The construction of the HADES underground research laboratory and its role in the development of the Belgian concept of a deep geological repository.

Mazurek, M., Oyama, T., Wersin, P., & Alt-Epping, P. (2015). Pore-water squeezing from indurated shales. Chemical Geology, 400, 106-121.

Mazurek, M., Wersin, P., Eichinger, F., Bath, A., Al, T., Clark, I. D., Kennell-Morrison L., Kampman N., & Traber, D. (2025). Techniques for porewater extraction from clayrocks. *Applied Clay Science*, *273*, 107855.

Moore, R. B., & Staubitz, W. W. (1984). *Distribution and source of barium in ground water at Cattaraugus Indian Reservation, southwestern New York* (No. 84-4129). US Geological Survey.

Musgrove, M. (2021). The occurrence and distribution of strontium in US groundwater. *Applied Geochemistry*, *126*, 104867.

Neeft E., Hoving A., Griffioen J., Behrends T., Vuorio M. & Ma M. (In preparation) Trace elements in Dutch Paleogene clays.

Robinet, J. C., Sardini, P., Coelho, D., Parneix, J. C., Prêt, D., Sammartino, S., ... & Altmann, S. (2012). Effects of mineral distribution at mesoscopic scale on solute diffusion in a clay-rich rock: Example of the Callovo-Oxfordian mudstone (Bure, France). *Water resources research*, *48*(5).

RWI, 2020. SGT-E3 Deep Drilling Campaign (TBO): Experiment Procedures and Analytical Methods at RWI, University of Bern (Rock-Water Interaction group, University of Bern, Switzerland Version 1.0, April 2020). Nagra Arbeitsbericht NAB 20-13, Nagra, Wettingen, Switzerland.

Sohrin, Y., & Bruland, K. W. (2011). Global status of trace elements in the ocean. *TrAC Trends in Analytical Chemistry*, *30*(8), 1291-1307.

Vardon, Philip J.; Abels, Hemmo A; Barnhoorn, Auke; Dieudonné, Anne-Catherine; Guy Drijkoningen et. al. (2024): Geothermal Project on TU Delft Campus - DAPGEO-02 Drilling Report. Version 4.

Verhoef, E., & Neeft, E. (2014, March). Status of R and D program on geological disposal of radioactive waste in the Netherlands. In Natural Analogues for Safety Cases of Repositories in Rock Salt. Salt Club Workshop Proceedings, 5-7 September 2013, Braunschweig, Germany (No. NEA-RWM-R--2013-10, pp. 66-74).

Wang, L., Honty, M., De Craen, M., & Frederickx, L. (2023). Boom Clay pore-water geochemistry at the Mol site: Chemical equilibrium constraints on the concentrations of major elements. *Applied Geochemistry*, *148*, 105541.

Wemaere, I., Marivoet, J., & Labat, S. (2008). Hydraulic conductivity variability of the Boom Clay in north-east Belgium based on four core drilled boreholes. *Physics and Chemistry of the Earth, Parts A/B/C*, *33*, S24-S36.

Wersin, P., Aschwanden, L., & Kiczka, M. (2024). Cation exchange parameters for Opalinus Clay and its confining units. *Applied Geochemistry*, *167*, 106003.
Wersin, P., Mazurek, M., & Gimmi, T. (2022). Porewater chemistry of Opalinus Clay revisited: Findings from 25 years of data collection at the Mont Terri Rock Laboratory. Applied geochemistry, 138, 105234.

Appendix

Chemical composition stainless steel used in high-pressure cell

Table S1. Chemical composition of the 316L stainless steel used in the high-pressure press at CIEMAT (wt%; Mott Corporation, Heat No. MMC 523).					
C %	**Ni %**	**Cr %**	**Fe %**	**Mo %**	**Si %**
0.024	11.034	16.340	Balance	2.240	0.798
Mn %	**Co** %	**Cu** %	**W** %	**S** %	**Nb** %
0.103	—	—	—	0.011	—
B %	**O** %	**P** %	**Other** %		
—	0.006	0.006	—		

Stable isotopes of pore water samples extracted by squeezing

Table S2. Stable isotopes in pore water samples extracted by squeezing (data provided by CIEMAT)			
Core*	Squeezing pressure (MPa)	$\delta^{18}O$ (‰ vs. VSMOW)	$\delta^{2}H$ (‰ vs. VSMOW)
C20	20	−3.69	−28.94
C57	20	−3.00	−23.17
C75	20	−3.05	−23.30

*C20, C57, and C75 refer to samples DAPGEO-02-C20, DAPGEO-02-C57, and DAPGEO-02-C75, respectively.

Test ^{81}BrH interference with ^{82}Se measurements using ICP-MS

Trace elements element analysis with ICP-MS is intrinsically prone to inferences between the target isotope of one element and isotopes with the same mass of other elements, element clusters forming in the plasma with the same mass and multiply charged ions with the same m/z ratio. In this study the ^{82}Se isotope was used for determining Se concentrations due to strong interferences with argides and dimers of the more prevalent isotopes $^{80}Se^+$ (e.g. $^{40}Ca^{40}Ca^+$, $^{40}Ar^{40}Ar^+$ $^{40}Ar^{40}Ca^+$) and ^{78}Se ($^{38}Ar^{40}Ar^+$ and $^{38}Ar^{40}Ca^+$). However, the strong correlation between Se and Br observed in all solutions created the suspicion that the Se concentrations were affected by interferences with Br. In particular the $^{81}BrH^+$ is known to interfere with ^{82}Se measurements using ICP-MS. For this reason we measured Br standard solutions with different concentrations in order to determine the corresponding ^{82}Se signal.

For this study Se concentrations were determined in the standard mode. With increasing Br concentration the signal obtained for m/z = 82 also increased proportionally resulting in corresponding detected Se concentrations around 13 ppm at Br concentrations of around 5700 ppm (Fig. S1). The measured Se concentrations in the diluted pore waters collected by high-pressure squeezing tend to be roughly about 10% higher than those resulting from $^{81}BrH^+$ interference at the corresponding Br concentrations.

In the test, it was also investigated whether $^{81}BrH^+$ interference can be reduced when measuring in collision mode with kinetic energy discrimination using He gas. However, the interference was about three times larger when using collision mode (data not shown).

Based on this test, it is suggested that the Se concentrations measured in the samples with saline matrix cannot be explained by $^{81}BrH^+$ interference alone and are significantly larger than zero. This implies that correction for $^{81}BrH^+$ interference could be possible but would result in large relative uncertainties in view of the broadness of the confidence interval of the linear regression line. However, in this stage, it is uncertain how reproducible the strength of the $^{81}BrH^+$ interference is, which could fluctuate among different sets of analyses depending on small changes in operational conditions. For this reason, we conclude that quantification of Se concentrations in the samples with saline matrix and high Br concentrations is unreliable based on the

collected data. Consequently, the reported Se concentrations were ignored in the report.

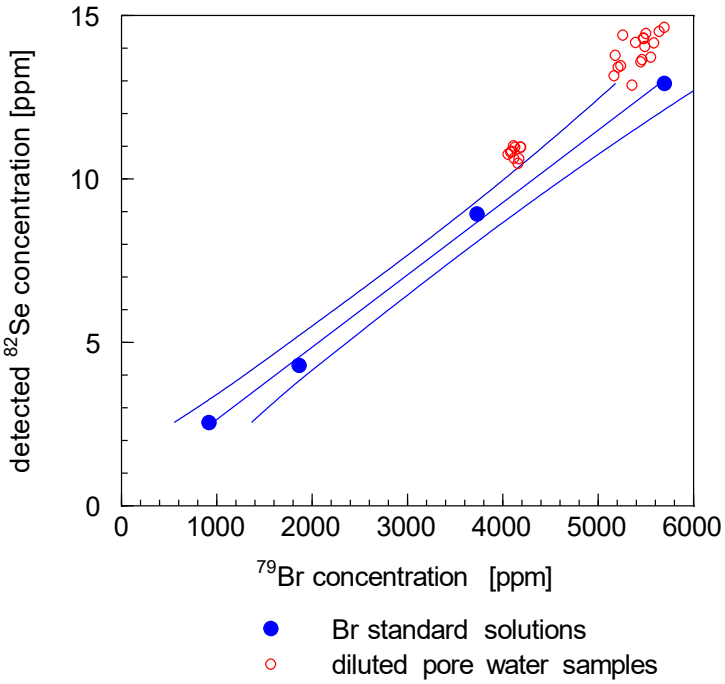

Fig. S1 Comparison between detected Se concentrations in 20 times diluted, squeezed pore waters based on the ^{82}Se isotope with the Se signal obtained when measuring Br standard solutions, as a function of Br concentrations measured in the form of ^{79}Br. The blue lines represent the linear regression for the Br standard solutions with the 95% confidence intervals.

Ciemat Report: Pore water samples for trace elements analysis from poorly indurated Neogene and Paleogene clays in the Netherlands

Ana María Fernández, L. Viviana Estrada, Paula Nieto (CIEMAT)

31/10/2025

Pore water samples for trace elements analysis from poorly indurated Neogene and Paleogene clays in the Netherlands

Ana María Fernández, L. Viviana Estrada, Paula Nieto (CIEMAT)

12/12/2025

Table 1. Physical parameters of the core samples.

Core Sample	DAPGEO-02-**C20**	DAPGEO-02-**C57**	DAPGEO-02-**C75**
Old Nomenclature (drilling report)	C20	C50	C58
Depth (m)	363.4-364.1	392.66-393.66	405.11-406.11
Date	23/03/2022	23/03/2022	23/03/2022
Formation	Breda	Dongen	Landen
Formation Member	Diessen	Ieper	Liessel
Dry density (g/cm^3)	1.70 ± 0.01	1.67 ± 0.02	1.49 ± 0.02
Water content (%)	22.1 ± 0.1	20.4 ± 0.7	28.7 ± 0.5

Table 2. Characteristics of the pore water squeezing tests.

Core sample	**Initial mass (g)**	**Initial w.c. (%)**	**Squeezing Pressure (MPa)**	**Time elapsed (days)**	**Water collected (mL)**	**Porewater extracted (mL)**	**Final w.c. (%)**	**F, Dry density (g/cm^3)**	**Final mass (g)**	**Efficiency (%) (1)**	**Total Efficiency (%) (2)**
C20	548.65	22.1	5-50	7	49.1	51.9	12.6	1.98	496.71	94.6	52.4
C57	554.34	20.4	5-50	14	30.6	49.0	12.2	1.96	505.30	62.4	52.2
C75	484.42	28.7	5-50	11	48.1	55.9	13.5	1.89	428.54	86.1	51.7

(1) Efficiency (%) = (Collected water x 100)/Extracted water;
(2) Total Efficiency (%) = (100 x extracted water)/(Initial mass – Dry mass)

Table 3. Pore water samples for Trace analysis sent to University of Utrecht.

Core sample	**P = 5 MPa**	**P = 20 MPa**	**P = 30 MPa**	**P = 40 MPa**	**P = 50 MPa**
C20	V= 5.6 mL / 56 µL HNO_3	V= 7.2 mL / 72 µL HNO_3	V= 8.3 mL / 83 µL HNO_3	V= 4.02 mL / 40 µL HNO_3	V= 3.36 mL / 40 µL HNO_3
C57	V= 5.74 mL / 57 µL HNO_3	V= 9.8 mL / 100 µL HNO_3	Not sampled	V= 5.15 mL / 50 µL HNO_3	V= 2.6 mL / 25 µL HNO_3
C75	V= 10.3 mL / 100 µL HNO_3	V= 6.2 mL / 62 µL HNO_3	V= 8.6 mL / 90 µL HNO_3	V= 0.9 mL / 9 µL HNO_3	V= 5.4 mL / 50 µL HNO_3

- Samples for chemical analysis and isotopes:

Table 4. Samples for chemical analysis and isotopes

Core sample	P = 10 MPa Chemical analysis	P= 20 MPa Isotopes
C20	11.5 mL	5 mL
C57	8.98 mL	5 mL
C75	11.59 mL	5 mL

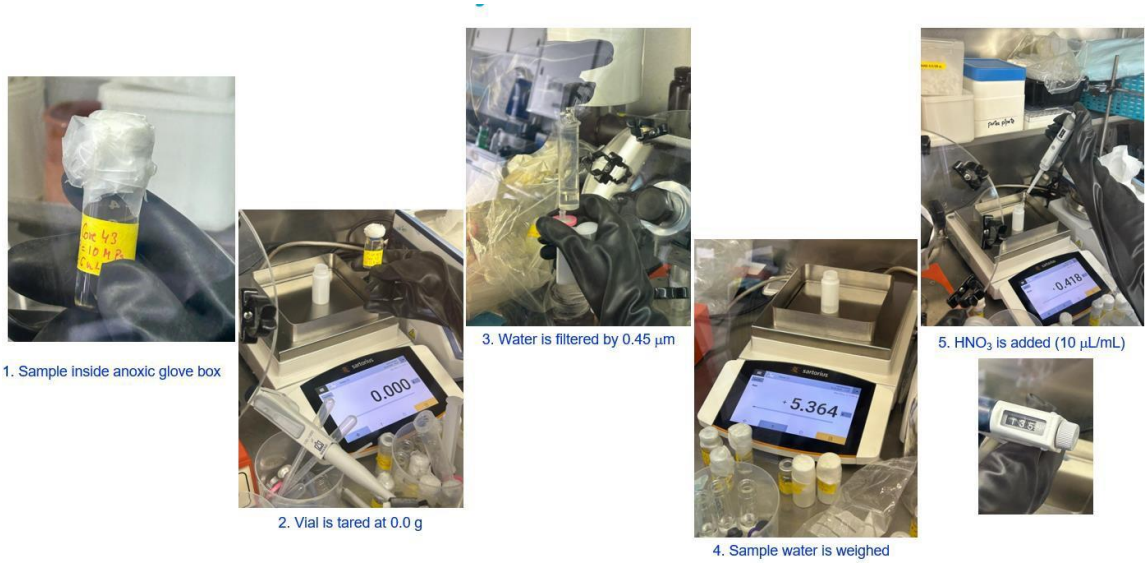

Figure 1. Acidification of the pore water sample after filtration by 0.45 µm for trace analysis.

Figure 2. Liquid and solid samples sent inside a refrigerated box for trace analysis.

Table 5. Stable isotopes in the pore water samples extracted by squeezing

Core sample	Formation, Member	Squezing pressure (MPa)	$\delta^{18}O$ (‰ vs, VSMOW)	$\delta^{2}H$‰ (‰ vs, VSMOW)
Core 20	Diessen F.	20	-3.69	-28.94
Core 57	Dongen F., Ieper M.	20	-3.00	-23.17
Core 75	Landen F., Liessel M.	20	-3.05	-23.30

Table 6. Stable isotope in the pore water samples extracted by squeezing

Formation	Diessen Formation		Dongen Formation, Ieper Member		Landen Formation, Liessel Member	
Sample	Core 20		Core 57		Core 75	
Depth (m.)	363.4-364.1		392.66-393.66		405.11-406.11	
Pressure (MPa)	10	20	10	20	10	20
Volume (mL)	11.5	5.0	9.0	5.0	11.6	5.0
pH	7.9	7.8	8.1	7.8	7.8	7.9
Alkalinity (meq/L)	3.89	3.83	2.83	1.83	2.39	2.27
HCO_3^- (mg/L)	237.4	233.6	172.7	111.6	145.8	138.5
TOC (mg/L)	--	23.7	87.4	49.2	47.2	24.1
F^- (mg/L)	<1	<1	<1	<1	<1	<1
Br^- (mg/L)	89	96	120	125	117	112
Cl^- (mg/L)	25000	21000	34000	27900	32000	26600
SO_4^{2-} (mg/L)	22	25	11.6	12.7	49	50
NO_3^- (mg/L)	<1	< 1	< 1	< 1	< 1	< 1
PO_4^{3-} (mg/L)	< 1	< 1	< 1	< 1	< 1	< 1
Al (mg/L)	< 0.6	0.29	< 0.6	0.95	< 0.6	0.44
Ca (mg/L)	810	820	1200	1100	1100	1100
Mg (mg/L)	610	640	940	880	780	830
Na (mg/L)	14000	12000	17000	17000	17000	16000
K (mg/L)	280	272	410	343	370	395
Sr (mg/L)	220	240	350	340	310	320
Fe (mg/L)	< 0.6	<0.2	< 0.6	<0.2	< 0.6	<0.3
Ba (mg/L)	6.6	6.7	10	10	10	11
B (mg/L)	16	18	16	16	18	21
Mn (mg/L)	< 0.6	0.3	< 0.6	0.3	0.88	0.72
Si (mg/L)	7.6	5.8	7.3	4.5	17.0	12
Ti (mg/L)	< 0.6	<0.2	< 0.6	<0.2	< 0.6	<0.3
V (mg/L)	< 0.6	<0.2	< 0.6	<0.2	< 0.6	<0.3
Zn (mg/L)	< 0.6	0.43	0.65	0.21	< 0.6	0.45

DAPGEO-02-C20 m. 363.4-364.1

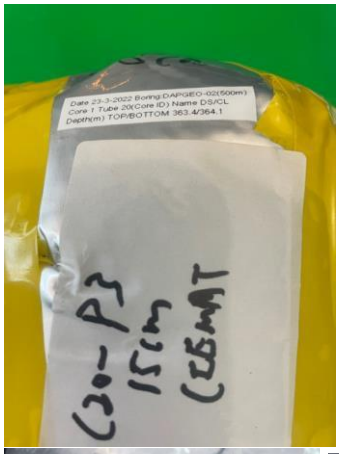

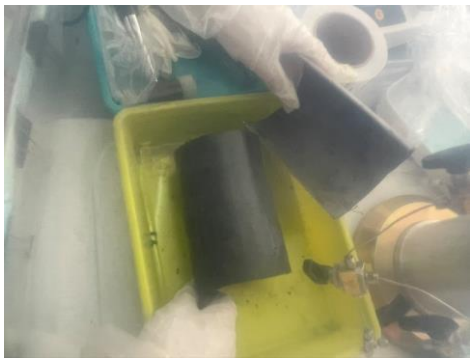

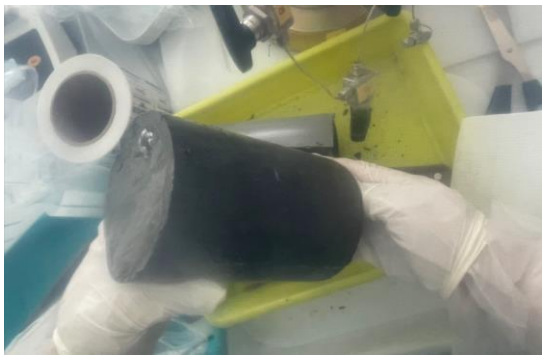

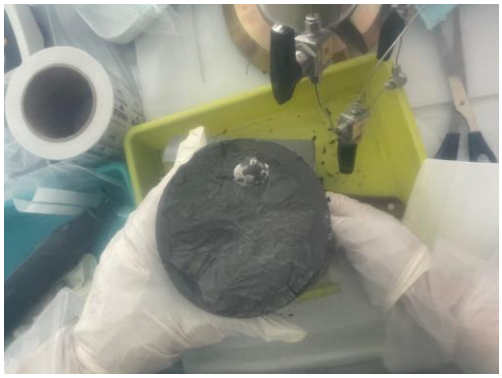

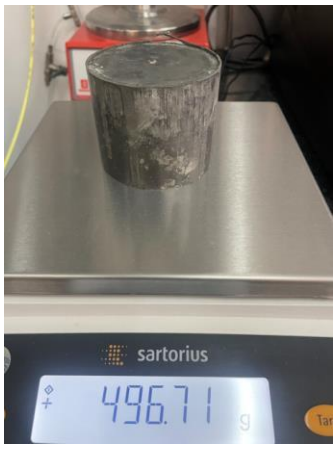

Initial sample

After Squeezing

DAPGEO-02-C57 m. 392.66-393.66

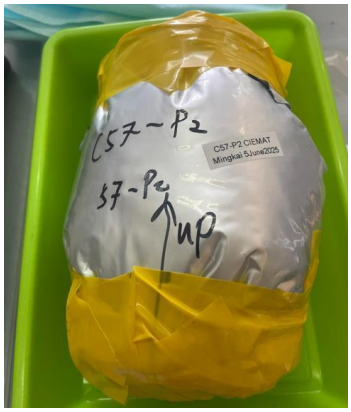




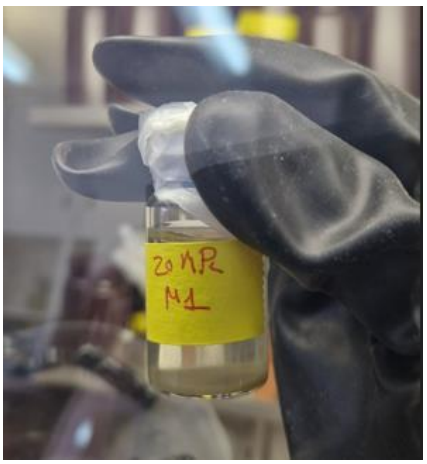

Initial sample After Squeezing

DAPGEO-02-C75 m. 405.11-406.11

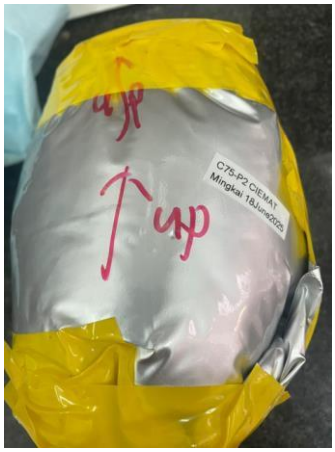





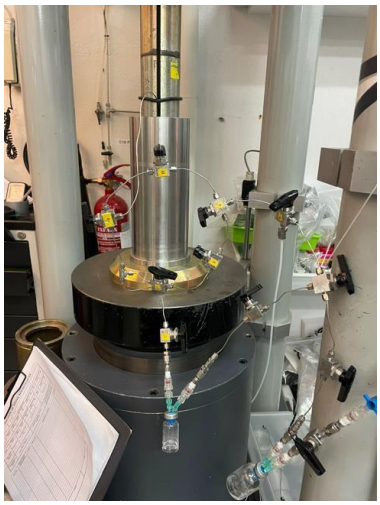

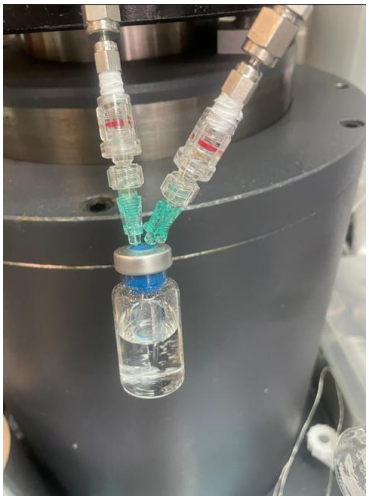

Initial sample After Squeezing